



BODIPY-based probes for fluorescence imaging of biomolecules in living cells

Journal:	<i>Chemical Society Reviews</i>
Manuscript ID:	CS-REV-01-2015-000030.R1
Article Type:	Review Article
Date Submitted by the Author:	08-Mar-2015
Complete List of Authors:	Kikuchi, Kazuya; Osaka University, Division of Advanced Science and Biotechnology Kowada, Toshiyuki; Osaka University, Chemical Imaging Techniques Maeda, Hiroki; Osaka University, Division of Advanced Science and Biotechnology

REVIEW ARTICLE

BODIPY-based probes for fluorescence imaging of biomolecules in living cells

Cite this: DOI: 10.1039/x0xx00000x

Toshiyuki Kowada,^a Hiroki Maeda^b and Kazuya Kikuchi*^{ab}Received 00th January 2012,
Accepted 00th January 2012

DOI: 10.1039/x0xx00000x

www.rsc.org/

Fluorescence imaging techniques have been widely used to visualize biological molecules and phenomena. In particular, several studies on the development of small-molecule fluorescent probes have been carried out, because their fluorescence properties can easily be tuned by synthetic chemical modification. For this reason, various fluorescent probes have been developed for targeting biological components, such as proteins, peptides, amino acids, and ions, to the interior and exterior of cells. In this review, we cover advances in the development of 4,4-difluoro-4-bora-3a,4a-diaza-5-indacene (BODIPY)-based fluorescent probes for biological studies over the past decade.

1. Introduction

Fluorescence imaging techniques are powerful tools for visualizing and analyzing the localization and dynamics of ions and biomolecules, such as amino acids and proteins, because of their high spatiotemporal resolution.^{1–4} Consequently, fluorescent proteins (FPs) are frequently used as fluorescent indicators or sensors, because functional FPs can easily be expressed with target proteins or peptides by introducing the genes encoding the fusion proteins.^{5–7} In addition, the localization of FPs can be controlled by genetic engineering.⁸ However, despite these advantages, there are some limitations.

^a Immunology Frontier Research Center (IFReC), Osaka University, Suita, Osaka 565-0871, Japan.

^b Graduate School of Engineering, Osaka University, Suita, Osaka 565-0871, Japan.

For example, there is a concern that the introduction of relatively large FPs in a fusion protein can interfere with the intrinsic function of the target protein. To overcome and resolve these issues, small molecule-based fluorescent probes have been considered as potential candidates.

The merits of small molecules against FPs are their smaller size, ease of functionalization, and availability of near-infrared (NIR) fluorescence.^{9,10} In addition, the timing for labeling target biomolecules can be controlled by the combination of small-molecule probes with bioorthogonal ligations^{11–15} or peptide or protein tags.^{16,17} For these reasons, a large number of small-molecule fluorescent probes have been developed.¹⁸ The most representative and widely used fluorophores are coumarin, fluorescein, BODIPY, rhodamine, and cyanine dyes (Fig. 1).^{19,20} Each fluorophore exhibits cyan to NIR fluorescence



Toshiyuki Kowada received his PhD degree from Kyoto University in 2010 under the supervision of Prof. Kouichi Ohe. After one year postdoctoral work with Prof. Kikuchi at Immunology Frontier Research Center (IFReC) in Osaka, he became a specially appointed assistant professor in Prof. Kikuchi's group. In 2014, he joined Prof. Jianghong Rao's group at Stanford University as a postdoctoral fellow. His research interest is in the development of small molecule-based functional probes for biological applications.



Hiroki Maeda received his bachelor degree in Engineering from Osaka University in 2011. He is continuing his studies at Osaka University under the direction of Professor Kikuchi in the area of chemical biology. His current PhD thesis focuses on the development of molecular imaging probes for clarifying cellular functions of bone metabolism in living mice. He was selected as a Research Fellow of the Japan Society for the Promotion of Science (JSPS) in 2014.

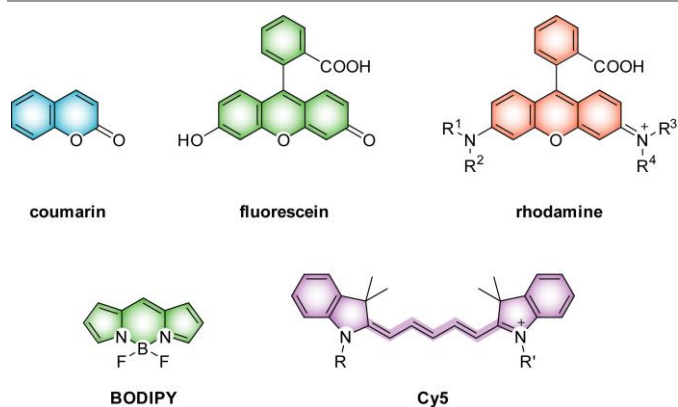


Fig. 1 Commonly used fluorophores.

based on its characteristic π -conjugated structure. Because of the usefulness of these fluorophores, various small molecule-based probes for cell/organelle staining and analyte sensing are commercially available. However, all of these fluorophores do not completely satisfy the required needs of probes; therefore, new probes are still being developed. In particular, when focusing on live-cell imaging, negatively charged fluorophores, typically fluorescein, often lack cell-membrane permeability, whereas they have decreased non-specific binding to cellular biomolecules. In contrast, rhodamine is a cationic dye that easily penetrates into cells and shows sufficiently high photostability. However, its cationic and hydrophobic characteristics can be problematic for cellular imaging, because rhodamines are prone to localize in the mitochondria or adsorb non-specifically to proteins or lipids.²¹ When shifting a target from cells to tissues or mice, NIR fluorescence with cyanine dyes is very useful, because NIR light can penetrate deep into tissues without significant damage or light scattering.²² In addition, the use of an NIR fluorophore can prevent the



Professor Kazuya Kikuchi graduated from the University of Tokyo (Japan) and did his postdoctoral training at UCSD with Prof Roger Y. Tsien (USA) and the Scripps Research Institute with Prof Donald Hilvert (USA). He was appointed as a research associate at the University of Tokyo (Japan) thereafter and promoted to associate professor.

He was appointed as a full professor at Osaka University in 2005. During these period he became involved in molecular imaging probes development for both fluorescence imaging and magnetic resonance imaging. He is focused both in *in vivo* imaging and single molecule cellular imaging. He had awarded IBM Science Award in 2008, JSPS prize in 2010, Chemical Society of Japan Research Award in 2011, and Inoue Science Award in 2012.

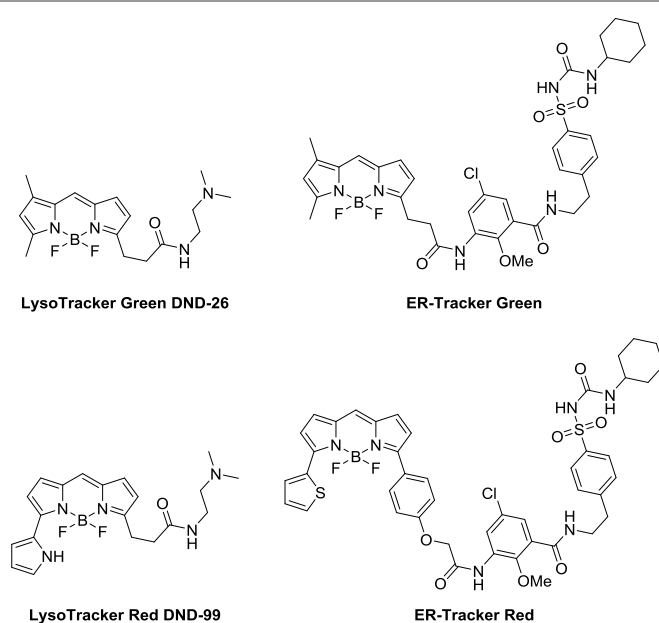


Fig. 2 Representative examples of commercially available BODIPY-based fluorescent probe.

interference of background signals derived from tissue autofluorescence. However, cyanine dyes exhibit lower photostability compared with rhodamine.

In these situations, BODIPY dye has been considered a potential scaffold for functional fluorescent probe development because of its relatively high photostability, neutral total charge, high fluorescence quantum yield, and sharp absorption and emission spectra.^{23–26} The fluorescence properties of BODIPY can be controlled by Förster resonance energy transfer (FRET)²⁷ or photo-induced electron transfer (PeT).^{28–30} Therefore, various BODIPY-based fluorescent probes have been developed. In addition, several probes are commercially available, including ER-Tracker Green and LysoTracker Red (Fig. 2).³¹ Nevertheless, BODIPY dye is highly hydrophobic, which is often problematic in the fluorescence imaging of biological samples. This review summarizes the current state of BODIPY-based probe development for application in fluorescence imaging. We omitted reports on the synthesis and physicochemical properties of BODIPY dye,^{23–25} as well as those on fluorescent metal sensors.³² Moreover, a recent review that summarizes the design and use of BODIPY-based fluorescent probes would also be helpful for readers.³³

2. Intracellular distribution of BODIPY

2-1. Organelle membrane

As described above, BODIPY dye is a neutral compound that can penetrate cell membranes. However, BODIPY dye tends to accumulate into subcellular membranes because of its relatively high lipophilicity.

As examples, compounds **1–3** were recently synthesized and appeared to be localized in the endoplasmic reticulum (ER) with negligible cytotoxicity (Fig. 3).³⁴ A co-staining experiment

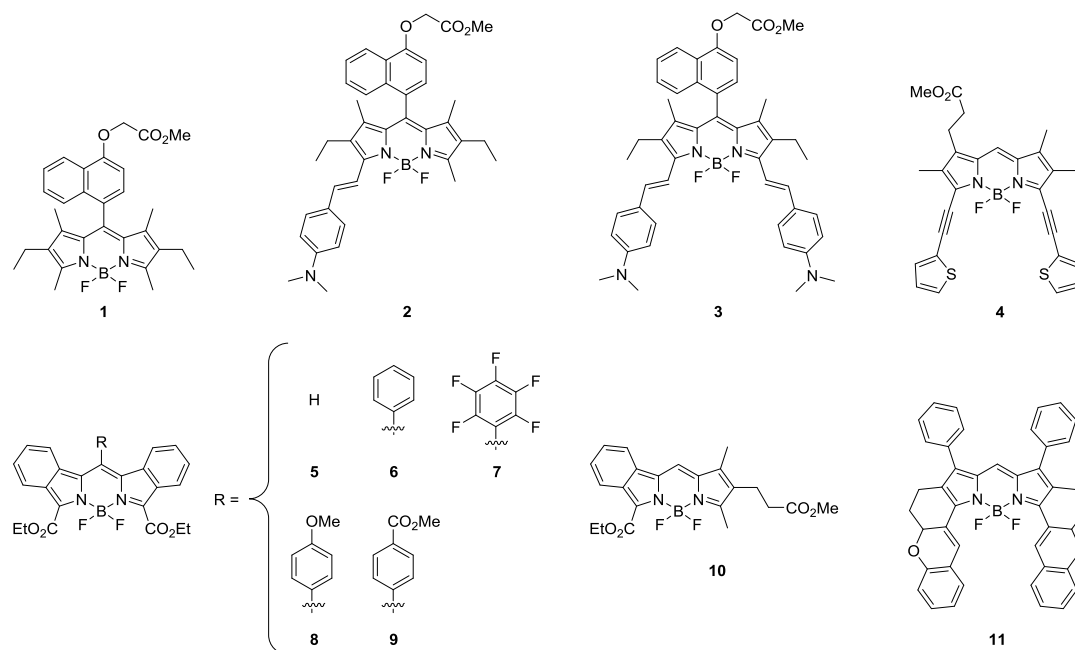


Fig. 3 Chemical structures of BODIPY-based probes with accumulation in the subcellular membrane.

with several organelle stains revealed that the fluorescence signals of compound **4** were mainly observed in the ER.³⁵ Benzannulated BODIPYs **5–10** also localized in the ER, as well as in the lysosomes, mitochondria, and Golgi apparatus.³⁶ Structurally-rigid NIR BODIPY **11** showed high photostability upon irradiation at 700 nm and little cytotoxicity to HepG2 cells.³⁷ The fluorescence signals of **11** appeared to be distributed throughout the cytoplasm, with a few punctate spots. These reports indicate that BODIPY dyes without any hydrophilic functionality exhibit membrane permeability, but cannot avoid localization into the intracellular membrane. Therefore, when aiming to visualize biomolecules in the cytosol or in particular organelles with reduced non-specific background signal, BODIPY dyes need to be modified with a hydrophilic group, such as carboxylate or ethylene glycol, or a targeting group for the organelle.

2-2. Cytosol

Since the aqueous solubility of compounds **1–11** is limited, it is possible that there is an unavoidable barrier for their practical use in biological imaging. Although the incorporation of an ionic substituent or bulky non-ionic polyethylene glycol moiety into a fluorophore has been utilized to enhance aqueous solubility, such modifications will also decrease cell membrane permeability. To overcome the poor water solubility, monoalkoxy BODIPYs **12** and **13** were developed (Fig. 4).³⁸ These monoalkoxy BODIPYs are readily accessible via a selective substitution of one fluorine atom in normal BODIPY dye.³⁹ Both **12** and **13** showed sufficient water solubility in PBS (24 and 122 μM , respectively) without any co-solvents or detergents. Their LogD values were determined to be 1.4 and 2.2, respectively, which are suitable for cell membrane

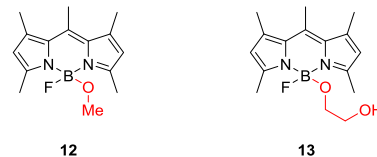


Fig. 4 Water-soluble BODIPYs with an alkoxy group on the boron atom.

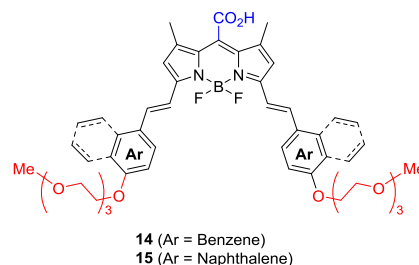


Fig. 5 BODIPY dyes with carboxylate and tetraethylene glycol groups.

penetration.⁴⁰ Moreover, their fluorescence properties were independent of pH changes to the solution. As a result of live-cell imaging, it was confirmed that both monoalkoxy BODIPYs can easily penetrate into cells, and the remaining probes inside of the cells can be washed out without any non-specific binding. On the other hand, Wu and coworkers reported an interesting relationship between lipophilicity and membrane permeability of BODIPY dye.⁴¹ BODIPY dyes **14** and **15** possess both anionic carboxylate and tetraethylene glycol groups (Fig. 5). Therefore, it was thought that these dyes could not penetrate cell membranes. However, surprisingly, compound **15** could enter and diffuse into cells, whereas no fluorescence signal was observed in HeLa cells treated with **14**. The exchange of benzene with naphthalene affected the cell membrane

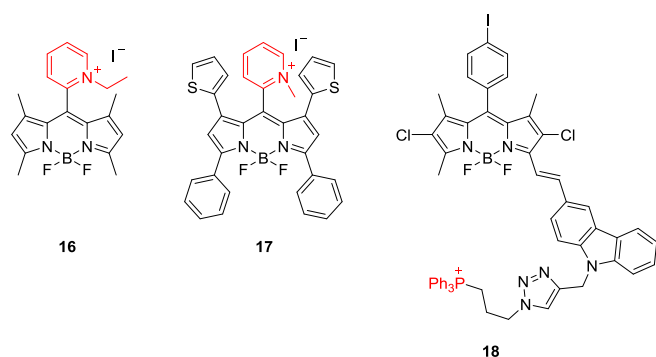
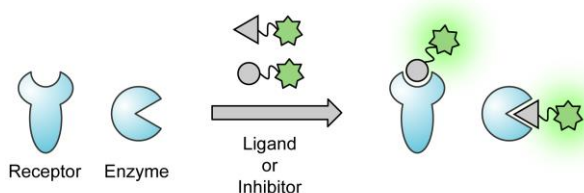
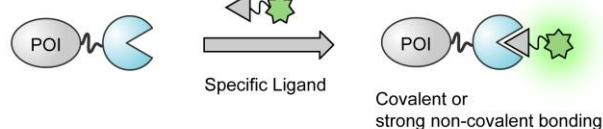


Fig. 6 Chemical structure of mitochondria-localized probes.

(A) Fluorescently labeled ligand or inhibitor



(B) Peptide or protein tag



(C) High-throughput screening

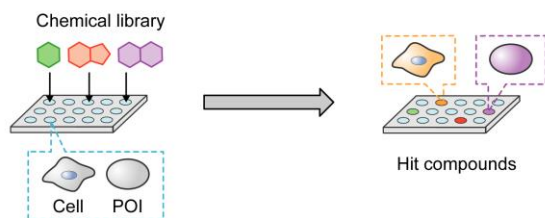


Fig. 7 Strategies for imaging target proteins.

permeability of the BODIPY dyes. This phenomenon demonstrates the importance of the balance between lipophilicity, hydrophilicity, and total charge of fluorophores for obtaining cell membrane permeability.

2-3. Mitochondria

In general, positively charged molecules tend to interact with and localize in negatively charged mitochondria.²¹ That is why commercially available MitoTracker dyes are usually composed of intrinsically cationic rosamine or rhodamine dye. In the case of neutral BODIPY dye, mitochondria-specific staining can be achieved by introducing a cationic moiety, such as an ammonium or phosphonium group (Fig. 6).^{42–44} Compounds **16**⁴² and **17**⁴³ contain a pyridinium moiety that facilitates increased water solubility as well as mitochondria-targeting

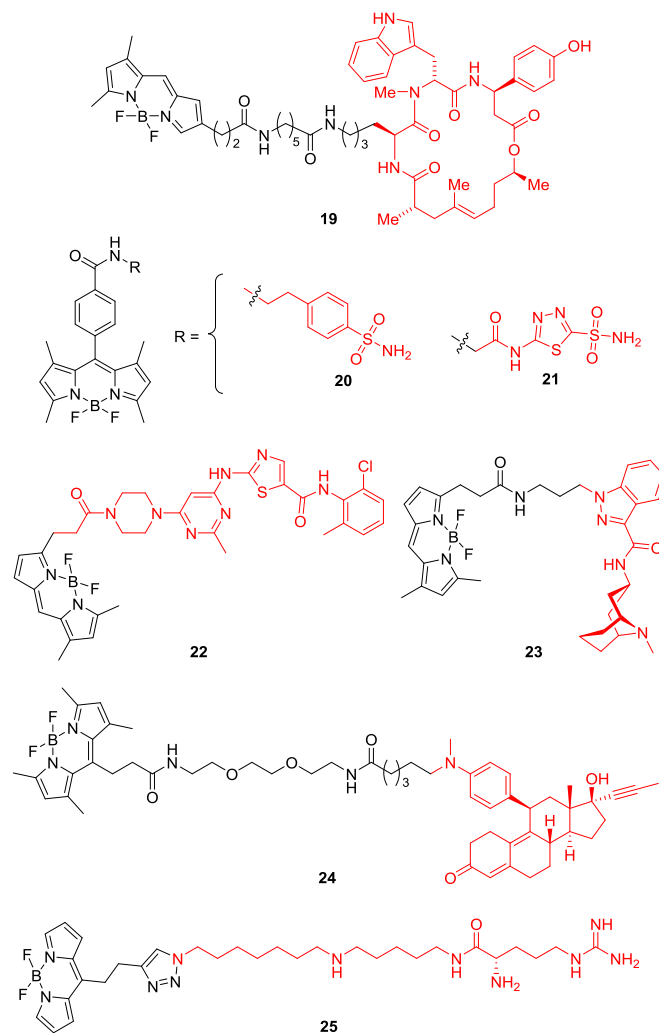


Fig. 8 BODIPY-based probes with high affinity to target proteins.

ability. These dyes show higher photostability than commercially available mitochondria stains. The phosphonium moiety also contributes to the retention of probe **18** in the mitochondria.⁴⁴ These cationic moieties can easily be obtained by straightforward conversion from their corresponding amine or phosphine. Therefore, it is expected that these mitochondria-targeting BODIPY dyes can be applied for understanding biological events in mitochondria, such as the signaling of reactive oxygen species (ROS),⁴⁵ by combination with a sensor moiety.

3. Imaging probes for target proteins

Many researchers have struggled to develop BODIPY-based probes for visualization of target proteins. To fluorescently label a target protein, there are several possible approaches (Fig. 7): A) conjugating a natural ligand or inhibitor for a target receptor or enzyme with a fluorophore, B) labeling a target protein fused with a peptide or protein tag,^{16,17,46} and C) high-throughput screening of various fluorescent molecules.⁴⁷

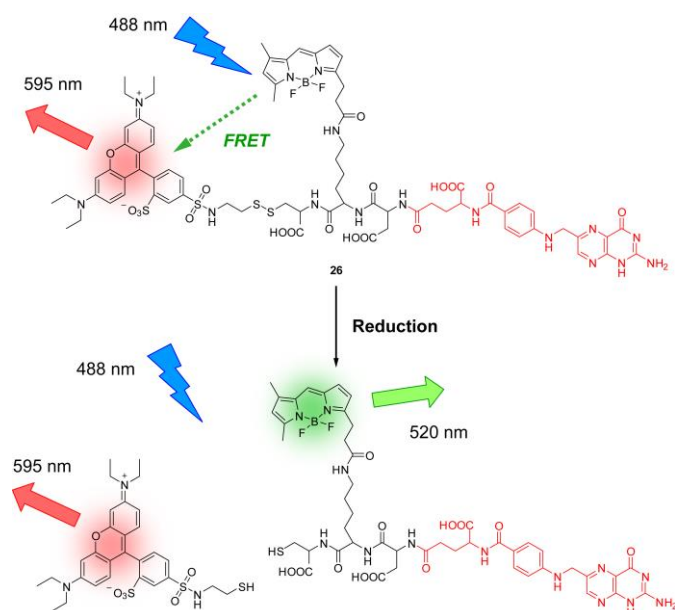


Fig. 9 Reduction-responsive FRET probe with folate.

3-1. Receptor ligands and enzyme inhibitors

When high-affinity molecules for targeting proteins are already known and readily available, modification of a receptor ligand with a fluorophore is a simple and reliable method for visualizing the localization of proteins of interest (POIs) (Fig. 7A). The important thing here is to understand the properties of fluorophores, ligands, and target proteins (e.g., the electronic charge and shape of the binding site) to avoid the loss of binding affinity.

The visualization of long-lived actin filaments in living cells was achieved using BODIPY-labeled jasplakinolide derivative **19**, which stabilizes F-actin (Fig. 8).⁴⁸ According to the study of structure-activity relationships, the modification of jasplakinolide with BODIPY dye at the position shown in Figure 8 should not affect its activity,⁴⁹ because the BODIPY dye may be located outside of the binding pocket.⁵⁰ To visualize tumor-associated carbonic anhydrases (CAs), a BODIPY fluorophore was conjugated with aromatic sulfonamides (**20** and **21**) (Fig. 8).⁵¹ These BODIPY-labeled sulfonamides showed comparable inhibitory activities with the CA inhibitor acetazolamide, as with several CA isozymes. Dasatinib-BODIPY **22** was synthesized to label a tyrosine kinase Src in Huh7 cells (Fig. 8).⁵² Although the 50% inhibitory concentration (IC_{50}) value of compound **22** to Src was 10-fold higher than that of dasatinib itself, **22** still had sufficient affinity for binding to Src. In compound **23**, an antagonist of the human serotonin receptor (5-HT₃AR), granisetron, was used (Fig. 8).⁵³ Even after conjugating BODIPY with granisetron, compound **23** showed comparably high affinity against 5-HT₃AR, resulting in achievement of its intracellular imaging with a highly diluted probe (10 nM) and short incubation time (10 min). The human progesterone receptor was imaged by compound **24**, in which the receptor antagonist, RU486 or Mifepristone, was conjugated with BODIPY through an

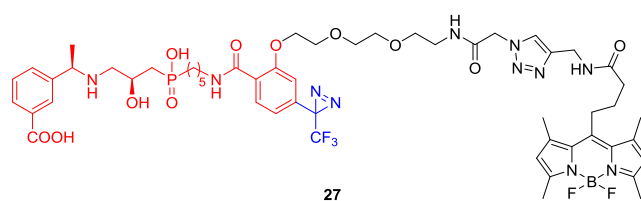


Fig. 10 Photoaffinity probe with BODIPY dye and GABA_B receptor binding group.

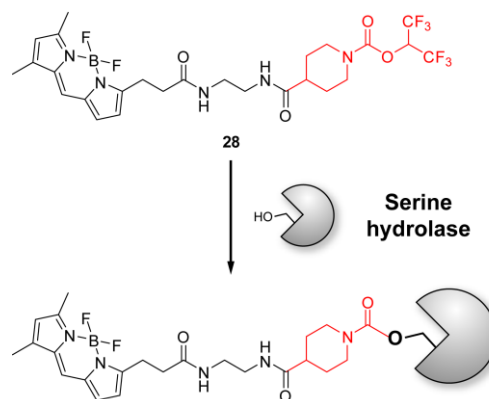


Fig. 11 Activity-based BODIPY probe for endocannabinoid hydrolases.

ethylene glycol linker.⁵⁴ Compound **25** is a fluorescent mimic of the natural product argitoxin-636, which is an inhibitor of the ionotropic glutamate (iGlu) receptor (Fig. 8).⁵⁵ *N*-Methyl-D-aspartate (NMDA) receptors, a subtype of the iGlu receptor family, could be visualized in hippocampal neurons with **25** because of its relatively high inhibitory potency to NMDA receptors, whereas the IC_{50} value of **25** is 2-fold higher than that of argitoxin-636.⁵⁶ Compound **26** possesses folate as a ligand for a folate receptor (FR) and reduction-responsive disulfide linker (Fig. 9).⁵⁷ Before binding to an FR, **26** showed red emission at 595 nm by FRET from BODIPY to rhodamine. During FR-mediated endocytosis, the disulfide bond in **26** was cleaved by reduction to release the rhodamine moiety and to produce green fluorescence.

To label the GABA_B receptor transiently expressed on the cell surface, probe **27**, which is composed of the antagonist for the GB1 subunit and trifluoromethylaryldiazirine moiety for photoaffinity labeling,^{58,59} was developed (Fig. 10).⁶⁰ It was confirmed that probe **27** has higher affinity to the GABA_B receptor than GABA, whereas the IC_{50} value of **27** is approximately 500-fold lower compared to that of the initial antagonist.⁶¹ In the cell labeling experiment, significantly higher fluorescence signals were observed with UV irradiation compared with the no UV irradiation condition. These results indicate that efficient labeling can be achieved with the combination of inhibitor and photoreactive group when the probe affinity to target proteins may be insufficient.

For labeling enzymes, particularly proteases, the concept of activity-based probes can be useful.^{62,63} To image the endocannabinoid hydrolases monoacylglycerol lipase (MAGL)⁶⁴ and α - β hydrolase-6 (ABHD6), Cravatt and coworkers developed an activity-based probe **28** (Fig. 11).⁶⁵

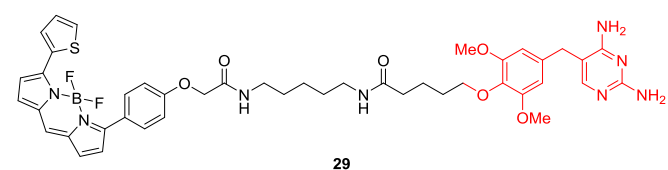


Fig. 12 BODIPY-based ligand for TMP-tag.

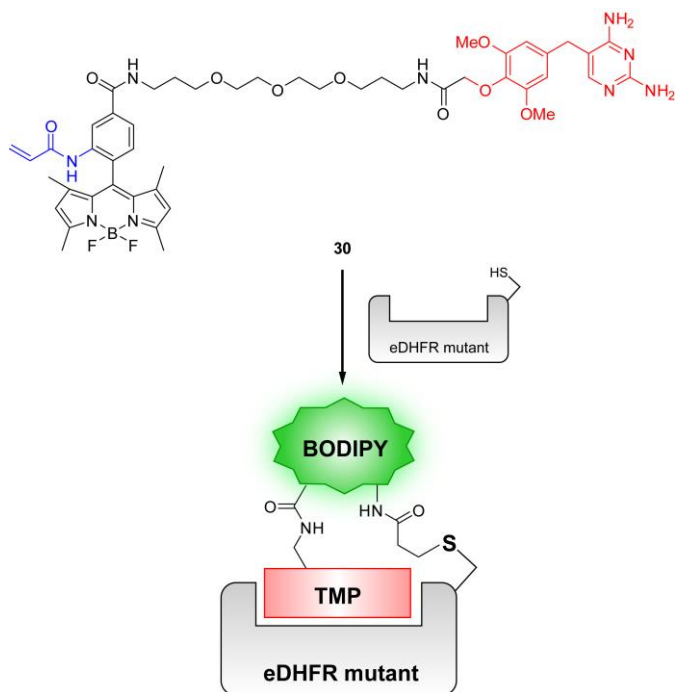


Fig. 13 Covalent labeling of the eDHFR mutant.

These serine proteases attack the *o*-hexafluoroisopropyl-activated carbamate, which was selected by comparing several leaving groups, to form a covalent bond with BODIPY dye through a linker. Gel analysis showed that **28** could not simultaneously distinguish between the two hydrolases, and labeled both proteins. Thus, in imaging experiments, selective inhibitors for each enzyme, JW951 for MAGL⁶⁵ and KT195 for ABHD6,⁶⁶ were used to visualize the distribution of the counterpart protein.

3-2. Peptide or protein tags

To specifically label target proteins, various protein or peptide tags that can form covalent bonds or tight non-covalent complexes with small-ligand molecules have been developed (Fig. 7B).^{16,17,46} The fusion protein of those tags with the POI can be genetically expressed in cells, so that its intracellular localization can be controlled using a subcellular localization signal, in a similar manner to fluorescent proteins.⁸

Cornish and coworkers reported that *Escherichia coli* dihydrofolate reductase (eDHFR) can be used as a small protein tag, using fluorophore-modified trimethoprim (TMP) as a ligand.⁶⁷ They synthesized TMP-BODIPY conjugate **29**, and achieved specific labeling of fusion proteins that are expressed on the plasma membrane or in the nucleus (Fig. 12). Wu and

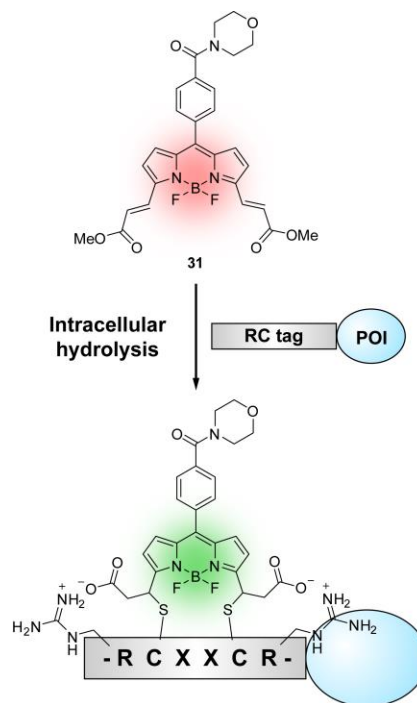


Fig. 14 Covalent bond formation and color change after labeling the RC tag-fusion protein.

coworkers introduced a mutation into eDHFR to construct a small protein tag that can covalently bind to fluorogenic BODIPY-based ligand **30** (Fig. 13).⁶⁸ The nucleophilic thiol group of a cysteine residue can attack the acrylamide group on BODIPY to form a covalent bond. Although the fluorescence enhancement of **30** is still low (2-fold) upon binding to the eDHFR mutant, the intracellular fluorogenic labeling method will be very useful for the detection of POIs with high sensitivity. Improvement of its fluorogenic properties is expected by exploring quenchers suitable to the BODIPY fluorophore.

A small peptide tag (RC tag) containing two pairs of Arg-Cys residues was developed for labeling intracellular target proteins.⁶⁹ This small peptide tag can covalently bind to the Michael acceptor, compound **31** (Fig. 14). After the coupling reaction, the emission color of **31** changed from orange to green, because the double bonds with BODIPY were converted to single bonds, leading to shortening of the π -conjugation length. The intracellular labeling of histone H2B with **31** was accomplished by double incorporation of the RC tag motif into its N-terminus.

One of the major advantages of peptide or protein tags over fluorescent proteins is the availability of functional probes, as well as their size. It is expected that utilization of photoactivatable small fluorophores, instead of photoactivatable fluorescent proteins, can prevent perturbation of protein function during tracking of a small number of target proteins. Consequently, photoactivatable BODIPY **32**, which possesses a dinitrobenzyl group as a caging moiety^{70,71} and benzylguanine for covalently bonding to a SNAP protein,⁷² was developed (Fig. 15).⁷³ The dinitrobenzyl group also functions as a

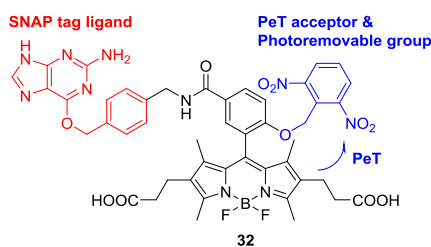


Fig. 15 Photoactivatable SNAP tag ligand.

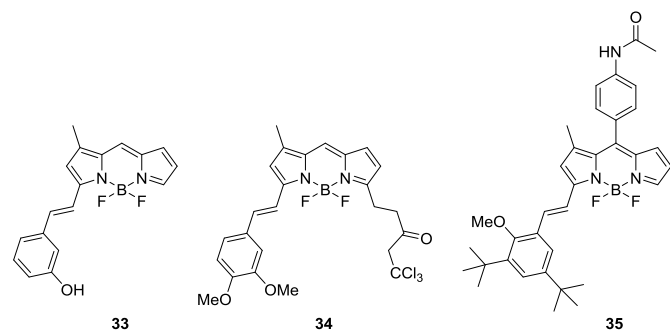


Fig. 16 Protein-binding probes developed through the DOFL approach.

fluorescence quencher via PeT. To demonstrate the validity of this system, EGFR- or H2A-SNAP fusion proteins were expressed in COS-7 cells or zebrafish embryos, respectively, and labeled with compound **32**.

3-3. Screening of potential candidates

If a receptor ligand is unknown or unavailable, high-throughput screening of various fluorescent molecules would be a better way to determine whether a fluorescent molecule can specifically label the target proteins or cells (Fig. 7C).⁴⁷

Chang and coworkers have enthusiastically developed BODIPY-based probes for fluorescence imaging through a diversity-oriented fluorescence library (DOFL) approach.^{47,74,75} From their library composed of 160 styryl-BODIPYs, compound **33** was found to have potential for detecting glucagon (Fig. 16).⁷⁶ Glucagon is a peptide hormone that is secreted from the intestinal L cells in response to low blood glucose levels.⁷⁷ The dissociation constant of **33** to glucagon was determined to be 13.3 μM , and its fluorescence quantum yield increased by about 13-fold after binding. An immunostaining experiment of mouse pancreas tissue sections revealed that **33** showed good co-localization with the glucagon antibody, indicating that this compound is a useful probe for glucagon-related biological studies.

The DOFL approach was also used to explore BODIPY-based fluorescent molecules for specific detection of neural stem cells (NSCs).⁷⁸ From screening 3160 compounds in E14-derived NSCs, mouse embryonic stem cells, astrocytes, and mouse embryonic fibroblasts, compound **34** was selected as the best compound for selectively and intensely staining NSCs (Fig. 16). The binding target of **34** was identified as fatty acid binding protein 7, with a dissociation constant of 9.6 μM .

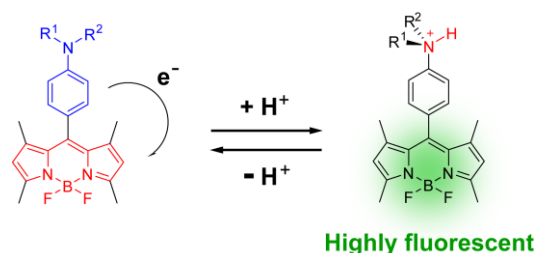


Fig. 17 pH-dependent fluorescence OFF-ON switching.

The fluorescent probe **35**, which is used for labeling beta cells in pancreatic islets of live animals, was also developed through the DOFL approach (Fig. 16).⁷⁹ The signal-to-background ratio reached a maximum after one hour. It was argued that compound **35** can be applied to fluorescence-guided surgery. As shown above, screening of a chemical library enables the discovery of potential candidates to specifically label a protein or cell of interest, even in cases in which an effective and reliable targeting moiety is unidentified or unavailable. By utilizing the screening results, key biomolecules necessary for selective imaging can be identified, and specific labeling probes can be developed by fine-tuning the probe structure.

4. pH sensor

While cytoplasmic pH is regularly maintained as neutral, a decreased pH value is observed in some organelles (endosomes: 5.5–6.3; lysosomes: 4.7) and some types of tumor tissues.⁸⁰ For visualization of these lower-pH compartments, BODIPY-based pH-sensitive fluorescent probes have been developed. In particular, a PeT mechanism is often used to introduce the fluorescence switching property of BODIPY dye (Fig. 17).^{81–83} Since the fluorescence OFF-ON switching depends on protonation of an amino group, reversible pH changes can be detected, which seems to be difficult in the case of detecting other biomolecules, except for metals.

The monoclonal antibody for the human epidermal growth factor receptor type 2 (HER2), trastuzumab, was conjugated with pH-sensitive BODIPY **36** (Fig. 18).⁸⁴ The pK_a value of **36** was determined to be 6.0, which was deemed suitable for selective imaging of acidic pH in lysosomes. After binding to HER2 on the cell surface, the trastuzumab-**36** conjugates were internalized via receptor-mediated endocytosis, leading to a gradual increase in punctate fluorescence spots inside of the cells. Moreover, this trastuzumab-**36** conjugate was also applicable in *in vivo* imaging of HER-2 positive tumors.

Bone-targeting pH-activatable probe **37** was developed to image bone-resorbing osteoclasts in live mice (Fig. 18).^{85,86} Compound **37** showed an almost identical pK_a value to that of compound **36**, indicating no effects of the tethered bisphosphonate group. After probe **37** was subcutaneously administered to mice, intense fluorescence between bone-resorbing osteoclasts and bone tissues was observed, because osteoclasts create an acidic compartment during bone resorption (Fig. 19).

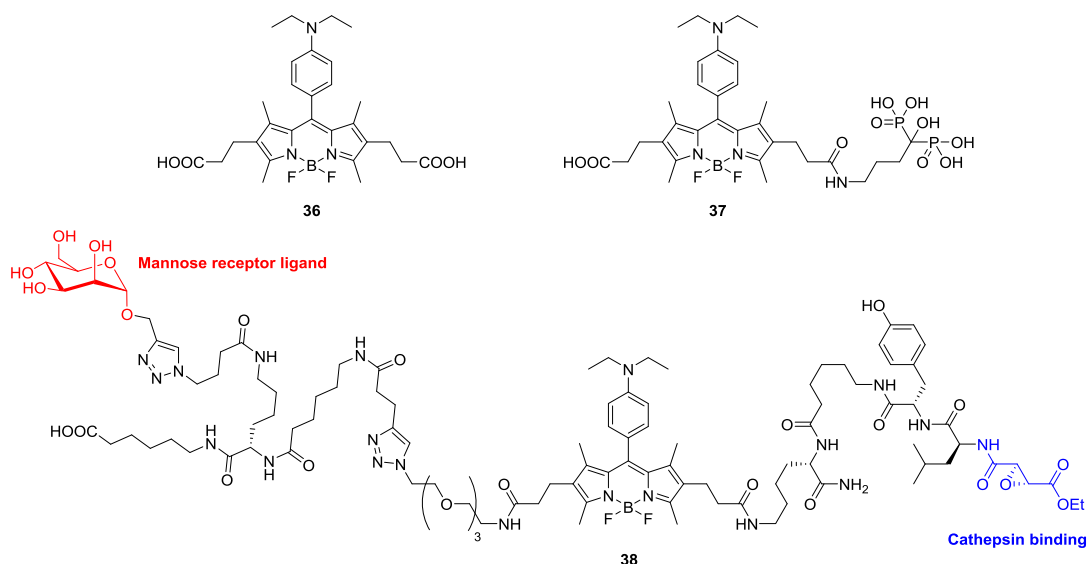


Fig. 18 pH-sensitive BODIPY probes.

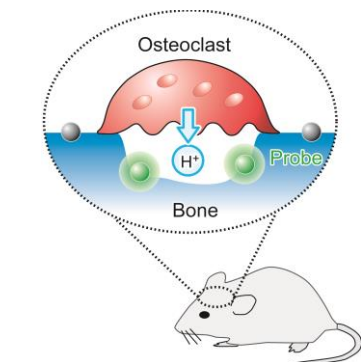


Fig. 19 In vivo fluorescence imaging of osteoclasts.

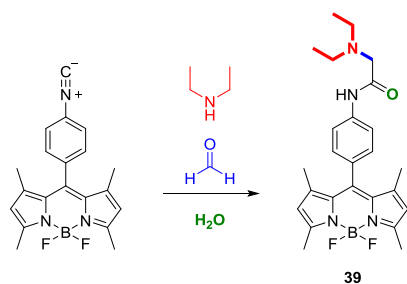


Fig. 20 Low-pH sensing probe developed via a multicomponent reaction.

To target cathepsins (lysosomal proteases), pH-sensitive BODIPY was conjugated with mannose as a ligand for a mannose receptor and epoxy-based cathepsin inhibitor (**38**, Fig. 18).⁸⁷ Despite having the same pH-sensitive aniline moiety as compounds **36** and **37**, compound **38** had a slightly lower pK_a value (5.1). This might be due to the protonation of the amino group being partially disturbed by encapsulation with relatively large and flexible functionalities extending in the lateral direction from the BODIPY core. This result implies that the entire molecular structure should be carefully considered when

designing PeT-based pH probes, rather than simple use of the same pH-sensitive moiety as reported. After entering the endosome, compound **38** covalently binds to cathepsins, through the nucleophilic addition of cysteine to the epoxy moiety.

Compound **39** was synthesized via a multicomponent reaction of isonitrile-BODIPY with formaldehyde and diethylamine (Fig. 20).⁸⁸ Its pK_a value was determined to be 5.76 ± 0.07 and is, thus, suitable for imaging the acidic environment in phagosomes. Visualization of phagocytic macrophages in zebrafish was accomplished by treating zebrafish larvae with compound **39**.

5. Thiols

Thiols play an important role in the formation and maintenance of the higher-order structure of proteins, as well as in the intracellular redox system.^{89,90} The major strategies to detect intracellular thiols include utilizing the nucleophilicity of thiols.⁹¹ There are, however, various other nucleophiles inside of cells, such as amines and alcohols, in lipids, amino acids, peptides, and proteins. Moreover, it is often necessary to selectively detect a specific thiol, (e.g., glutathione) from several biological thiols.

5-1. Nucleophilic aromatic substitution

The 2,4-dinitrobenzenesulfonyl (DNBS) group is an effective

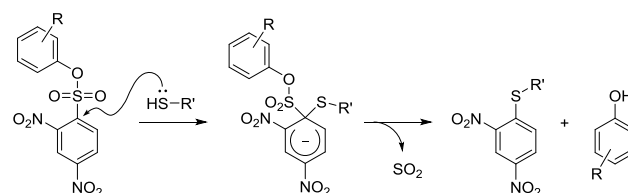


Fig. 21 Thiol detection via S_NAr reaction of a DNBS group.

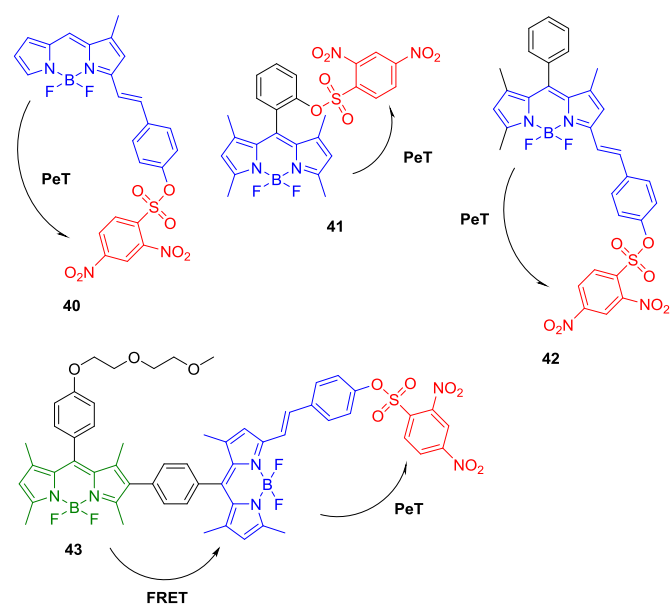


Fig. 22 Thiol-sensitive probes with a DNBS group.

quencher for the BODIPY fluorophore, and is also a protecting group that can be removed by S_NAr reaction with nucleophilic thiols (Fig. 21). Compound **40** exhibited remarkable fluorescence enhancement (25-fold) upon reaction with cysteine (Fig. 22).⁹² However, other thiols, such as thioglycol, glutathione, and thiophenol, were also reactive with **40** and similarly enhanced fluorescence. Compound **41** also possessed a DNBS group as a PeT quencher and a cysteine-reactive group (Fig. 22).⁹³ The selectivity to other thiols was investigated, and thioglycolic acid and glutathione showed 2-fold and 10-fold lower fluorescence enhancement upon reaction with cysteine, respectively. Both compounds **42** and **43** were developed to detect cysteine in cells using a DNBS moiety with negligible reactivity to glutathione (Fig. 22).^{94,95}

Nucleophilic substitution of chloro- or nitrothiophenyl-substituted BODIPY can be used to detect thiols. In particular, ratiometric imaging of glutathione was performed using chlorinated BODIPY **44** (Fig. 23).⁹⁶ The monochlorinated BODIPY **44** reacted with thiols, such as cysteine, homocysteine, and glutathione, to form thioethers. In the cases of cysteine and homocysteine, intramolecular replacement of the thiolate group with an amine produced aminated BODIPY **45**.^{97,98} In contrast, glutathione did not produce the aminated BODIPY, because of the lack of a nucleophilic amine at the appropriate position for intramolecular S to N rearrangement. In addition, thioether **46** showed intense fluorescence at 588 nm, whereas the fluorescence intensity of aminated BODIPY **45** was much lower and/or blue-shifted. Therefore, glutathione can be discriminated from cysteine and homocysteine by the different spectrum changes of **44** upon reacting to thiols. In a similar manner to **44**, the nitrothiophenol-substituted BODIPY **47** reacted with thiols to show a turn-ON fluorescence response, because the leaving group, 4-nitrothiophenol, can act as a fluorescence quencher. (Fig. 24).⁹⁹

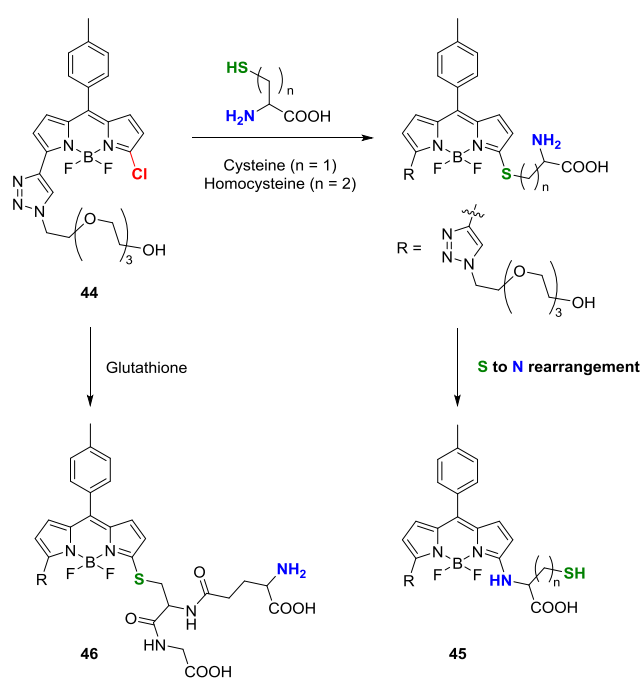


Fig. 23 Reaction between chlorinated BODIPY and thiols.

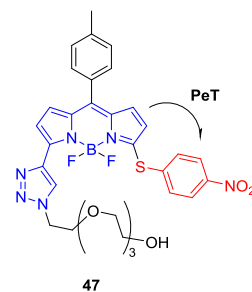


Fig. 24 Thiol-responsive nitrothiophenol-substituted BODIPY.

5-2. Michael addition

Michael addition of thiols can be useful for detecting intracellular thiols, because the double bond in fluorophores can be converted to a single bond, leading to changes in their photophysical properties. In the case of compound **48**, the amine of cysteine or homocysteine reacted with the carbonyl group to form an intermediate imine, and intramolecular cyclization then occurred (Fig. 25).¹⁰⁰ The reaction product showed 45-nm blue-shifted fluorescence at 567 nm. In addition, glutathione showed no reactivity to compound **48**.

Akkaya and coworkers reported a fluorescent probe for detecting glutathione with a combination of Michael addition and modulation of PeT quenching.¹⁰¹ Compound **49** was composed of nitroolefin as a Michael acceptor and aza-crown ether-based aniline as a PeT donor (Fig. 26). After the addition of glutathione to nitroolefin, the protonated amine of glutathione was appropriately arranged to interact with the aza-crown ether, resulting in significant fluorescence enhancement at 518 nm. When cysteine or homocysteine was conjugated with **49**, the distance between the terminal sulfur atom and the

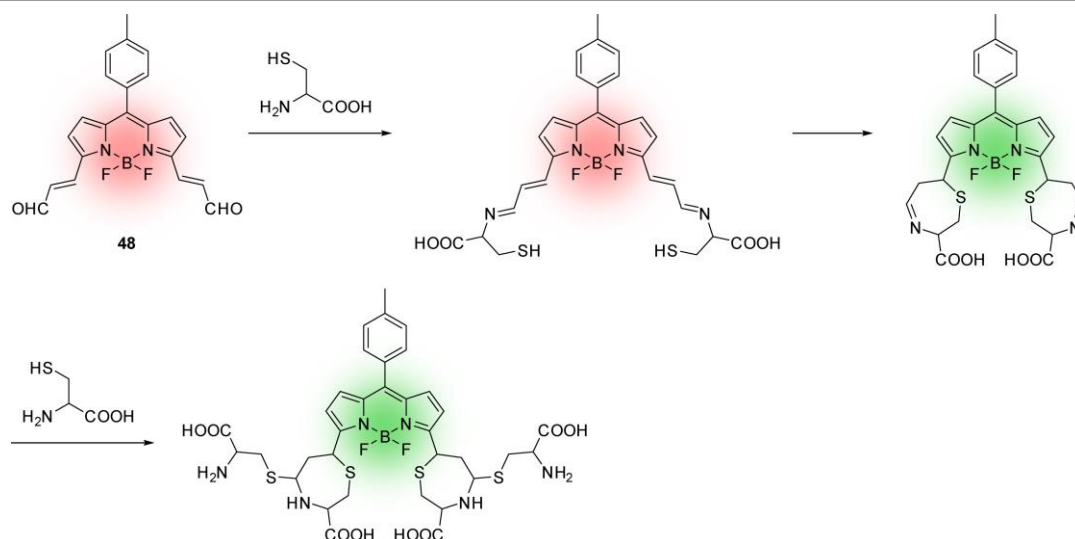


Fig. 25 Plausible reaction mechanism for the reaction of compound **48** with cysteine.

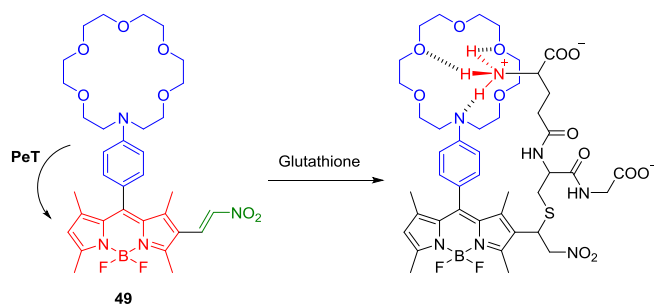


Fig. 26 Glutathione probe with crown ether and nitroolefin.

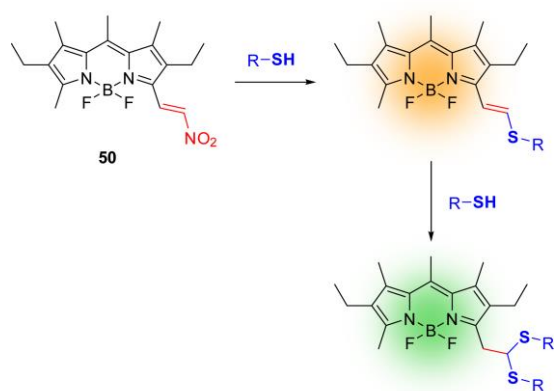


Fig. 27 Reaction of nitroolefin **50** with thiols.

protonated nitrogen was somewhat shorter for the interaction with the aza-crown ether. Hence, for these thiols, the fluorescence enhancement was much lower compared to glutathione.

Although compound **50** apparently includes the nitroolefin moiety as a Michael acceptor, nucleophilic addition with thiols occurs at the α -carbon of the nitro group (Fig. 27).¹⁰² Before the thiol addition, compound **50** showed almost no fluorescence,

due to the intramolecular charge transfer from BODIPY to the nitroolefin moiety. Interestingly, significant fluorescence enhancement was observed by a reaction of **50** with cysteine, whereas other amino acids and glutathione barely reacted with **50**.

5-3. Transthioesterification

FRET-based probe **51** can be used for ratiometric detection of thiols in living cells (Fig. 28).¹⁰³ Before reaction with thiols, compound **51**, which is derived from rhodamine, showed fluorescence at 590 nm. A thiol can attack the carbonyl carbon of thioester to remove rhodamine from BODIPY in a similar manner to native chemical ligation.¹⁰⁴ A fluorescence increase at 510 nm and a decrease at 590 nm were observed by adding cysteine, homocysteine, and glutathione.

6. Gaseous molecules

Hydrogen sulfide (H_2S), nitric oxide (NO), and carbon monoxide (CO) are endogenously produced and act as gaseous signaling molecules.^{105–107} These gaseous molecules in cells can be visualized by appropriately selecting the reactive moiety for each molecule.

6-1. H_2S

Compound **52** selectively reacted with H_2S to form compound **53** and showed turn-ON fluorescence, probably due to the inhibition of PeT (Fig. 29).¹⁰⁸ Since the reaction mechanism can be the Michael addition of H_2S to methyl acrylate and subsequent formation of hemithioacetal, H_2S can preferentially react with **52** compared with other biorelevant thiols, such as cysteine and glutathione. Live-cell imaging of H_2S production was achieved by the addition of cysteine or glutathione, which can be enzymatically converted to H_2S in **52**-treated HeLa cells.¹⁰⁹

In a similar manner to the thiol detection in Section 5, the

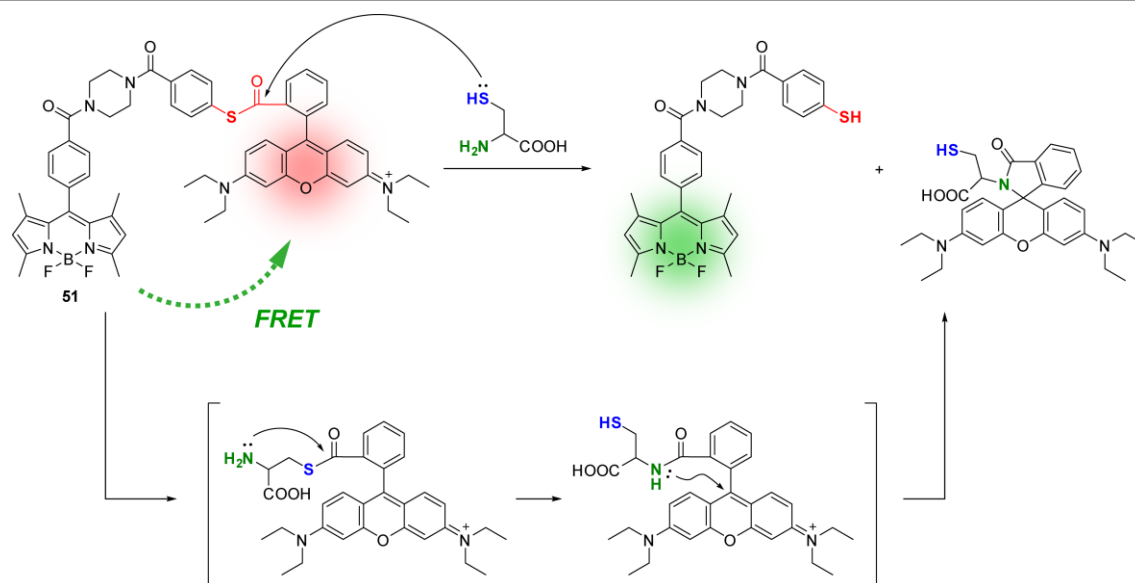


Fig. 28 Thiol-responsive FRET probe based on native chemical ligation.

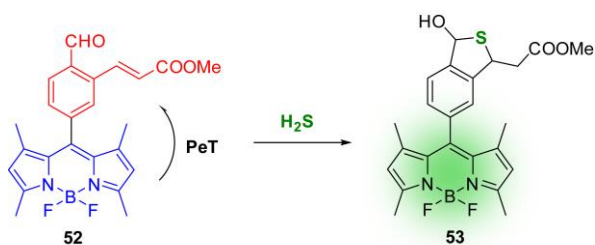


Fig. 29 H₂S-selective fluorescent probe.

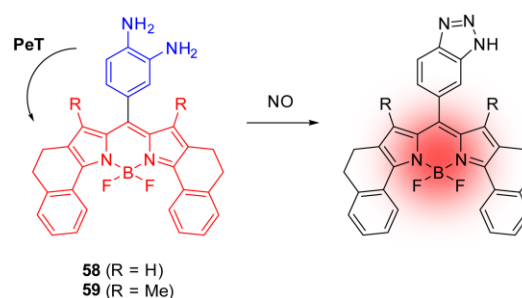


Fig. 32 NO-responsive probes based on benzotriazole formation.

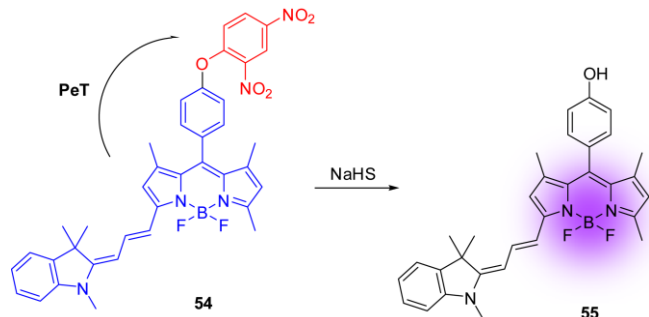


Fig. 30 H₂S probe with a DNB group as a quencher.

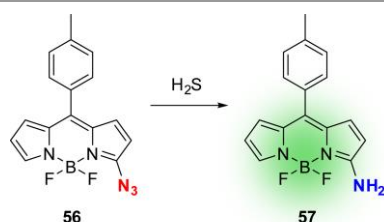


Fig. 31 H₂S probe based on the reduction of azide to amine.

nucleophilic substitution of electron-deficient dinitrobenzene (DNB) can be used to detect H₂S in living cells (Fig. 30).¹¹⁰

Before reaction with H₂S, NIR fluorescent molecule **54** showed almost no fluorescence, because of the quenching via PeT by the DNB moiety. It was confirmed that compound **55** was obtained by the reaction of **54** and H₂S, generating 18-fold fluorescence enhancement. Compound **54**-pretreated MCF-7 cells were incubated with H₂S, resulting in intense fluorescence in the mitochondria.

H₂S acts as both a nucleophile and as a reducing agent. Thus, the H₂S-mediated reduction of azide to amine^{111,112} can be used for the development of a turn-ON fluorescent sensor of H₂S.¹¹³ The absorption spectrum of azide **56** dramatically changed in response to an increasing concentration of H₂S (Fig. 31). In addition, the fluorescence intensity at 520 nm significantly increased upon H₂S addition. The transformation of compound **56** to **57** also occurred in live HeLa cells, and produced intense fluorescence.

6-2. NO

The *o*-phenylenediamine moiety plays a powerful role both as a reactive site for NO and as an electron donor in PeT quenching.¹¹⁴ Therefore, to image NO in cells and tissues, the NO-sensitive group was incorporated into NIR-fluorescent BODIPY **58** and **59** (Fig. 32).¹¹⁵ These probes showed over

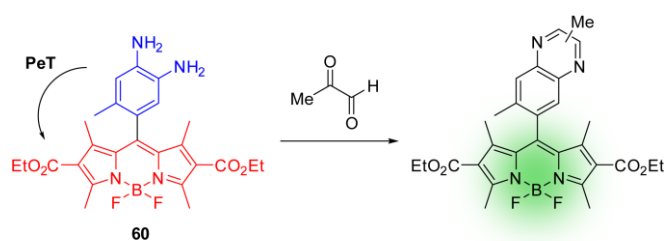


Fig. 33 Methylglyoxal-responsive probe.

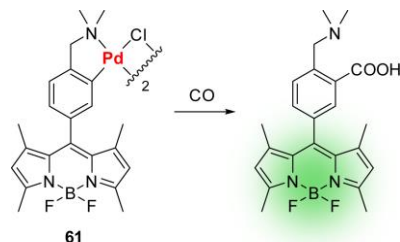
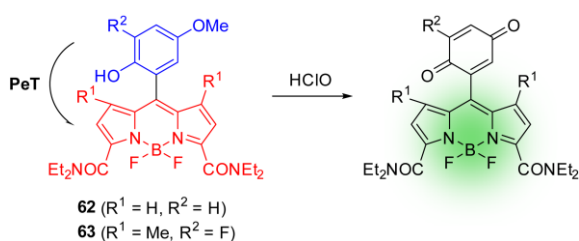


Fig. 34 CO-responsive probe based on quenching via the heavy-atom effect of palladium.

Fig. 35 Fluorescent probes for HClO detection based on transformation of *p*-methoxyphenol to benzoquinone.

400-fold fluorescence enhancement in response to reaction with NO, and the detection limit of NO was determined to be 2.1 nM and 0.6 nM for **58** and **59**, respectively. For NO imaging in living cells, the cells were treated with 1-hydroxy-2-oxo-3-(3-aminopropyl)-3-methyl-1-triazene as a NO donor after incubation with the NO probes. Both NO probes were membrane-permeable and showed NO-responsive turn-ON fluorescence inside of cells without any cytotoxicity. NO production in lung tissue inflammation was visualized by intraperitoneal injection of the probes. On the other hand, Spiegel and coworkers utilized the *o*-phenylenediamine moiety as a reactive group toward methylglyoxal rather than NO (Fig. 33).¹¹⁶ Compound **60** showed no NO-responsive turn-ON fluorescence, because triazole as a product can still work as an electron donor for PeT quenching. In contrast, since the quinoxaline does not have the ability to work as a quencher, compound **60** selectively showed turn-ON fluorescence to methylglyoxal, but not to NO.

6-3. CO

To selectively image CO in living cells, Chang and coworkers used the palladium complex **61** (Fig. 34).¹¹⁷ The fluorescence of **61** was quenched by the heavy-atom effect of palladium. After reaction with CO, the palladium atom was released from

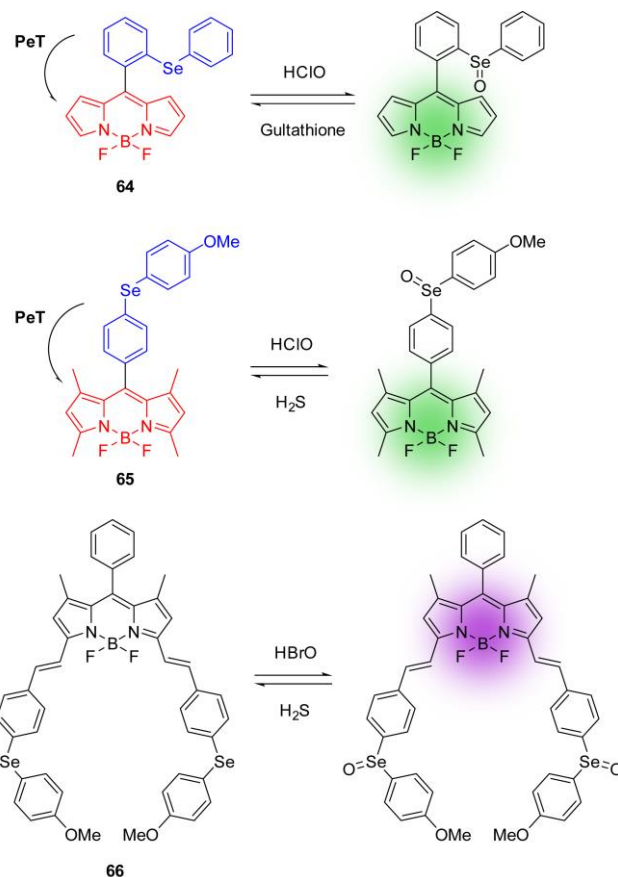


Fig. 36 Fluorescent probes for HClO or HBrO detection based on oxidation of selenide.

BODIPY, leading to fluorescence recovery. The fluorescence turn-ON response was selective to CO, and was barely affected by ROS or reactive nitrogen species (RNS).

7. ROS/RNS

ROS/RNS are involved in intracellular signaling, regulation of gene expression, and host defense from microbial infection.^{118,119} Recently, various BODIPY-based fluorogenic probes for the selective detection of ROS/RNS have been developed.

7-1. Hypochlorous (HClO) and hypobromous acid (HBrO)

HClO can be visualized by the oxidation of *p*-methoxyphenol to benzoquinone (**62** and **63**, Fig. 35),^{120,121} and diphenyl selenide to selenoxide (**64** and **65**, Fig. 36),^{122,123} because of the modulation of PeT quenching. Compounds **62** and **63** showed 1079-fold and 908-fold fluorescence enhancement upon reaction with HClO, respectively, whereas the other ROS did not induce such an enhancement. Lipopolysaccharide/interferon- γ (LPS/IFN- γ)- and phorbol myristate acetate (PMA)-induced HClO generation in cells was visualized using these probes.

After oxidation of selenide (**64** and **65**), an electron cannot transfer from selenoxide to the BODIPY core, because the

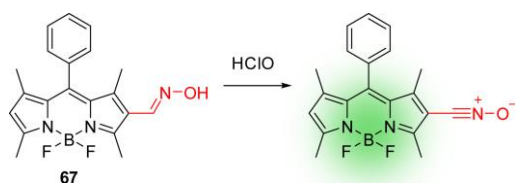


Fig. 37 Aldoxime-based probe for HClO detection.

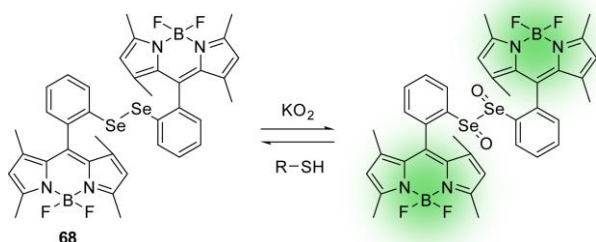


Fig. 38 Diselenide-based probe for $O_2^{\bullet-}$ detection.

HOMO energy level of the selenoxide is lower than that of both selenide and the BODIPY unit. In addition to their high selectivity to HClO among various ROS and RNS, the resulting selenoxides can be reduced to their initial selenides by glutathione or H_2S . Similarly, the HBrO-selective probe **66** was developed based on the redox system of selenide.¹²⁴

As another detection mechanism of HClO, the oxidation of aldoxime to nitrile oxide can be used (Fig. 37).¹²⁵ It was suggested that the significantly reduced fluorescence of compound **67** might be due to non-radiative decay via isomerization of the aldoxime group. The aldoxime **67** was membrane-permeable and showed HClO-responsive fluorescence enhancement in living cells.

7-2. Superoxide ($O_2^{\bullet-}$)

Diselenide **68** was selectively oxidized to diselenoxide by $O_2^{\bullet-}$, leading to remarkable fluorescence enhancement, due to inhibition of PeT from the selenium atom (Fig. 38).¹²⁶ In addition, diselenoxide was reduced to compound **68** with various thiols, such as glutathione and cysteine. Intracellular $O_2^{\bullet-}$ production was imaged by incubation of **68** with PMA-pretreated cells.

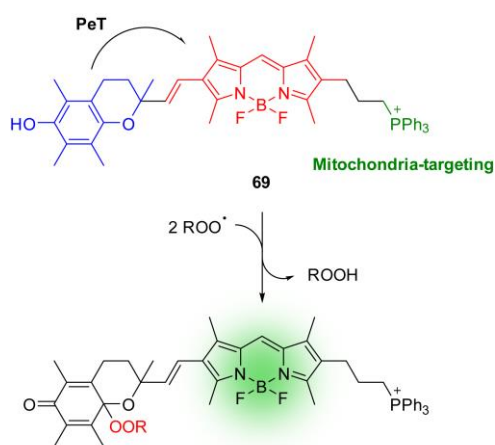


Fig. 39 ROO^{\bullet} -sensitive probe with a mitochondria-targeting group.

7-3. Peroxy radical (ROO^{\bullet})

Cosa and coworkers synthesized chromanol-modified BODIPYs for imaging lipid ROO^{\bullet} (Fig. 39).^{127,128} Compound **69** possesses a triphenylphosphonium moiety for targeting mitochondria. Chromanol is a partial structure of α -tocopherol, which is an antioxidant and effective radical scavenger. While the fluorescence of **69** was quenched by PeT from the chromanol moiety, the chromanone moiety was formed after scavenging ROO^{\bullet} , and hardly quenched the BODIPY fluorescence.¹²⁹ Moreover, fluorescence enhancement of **69** was observed in response to ROS production in the mitochondria, and was induced by treatment with methyl viologen.

7-4. Peroxynitrite ($ONOO^-$)

Intramolecular oxidation of phenol via a dioxirane intermediate can be used to detect $ONOO^-$ (Fig. 40).^{130,131} The fluorescence turn-ON response (69-fold) of **70** upon reaction with $ONOO^-$ was controlled by PeT.¹³² The endogenous $ONOO^-$ production was visualized by LPS/IFN- γ - and PMA-stimulation of **70**-treated macrophages.

8. Cellular viscosity

Increased intracellular viscosity interferes with the diffusion of cellular materials, such as signaling molecules, enzymes, and short-lived intermediates, leading to cellular dysfunction and disease.¹³³ Intracellular viscosity changes can be visualized

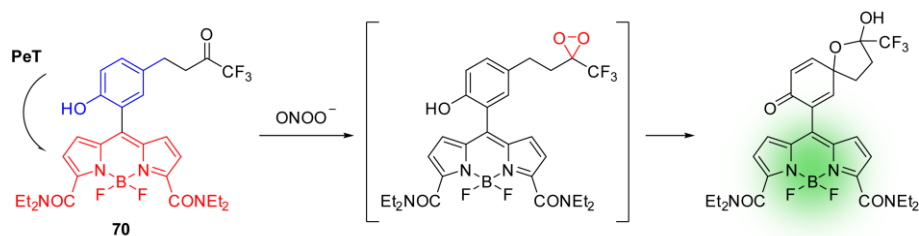


Fig. 40 BODIPY-based probe for $ONOO^-$ detection.

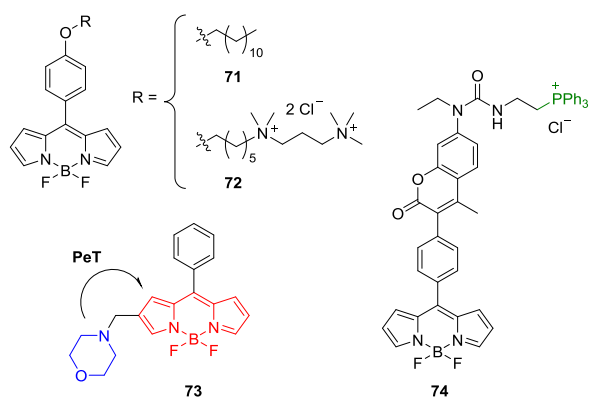


Fig. 41 BODIPY-based viscosity probes.

using BODIPY-based viscosity probes, of which photophysical property changes are induced by the restriction of bond rotation at the meso-position in a highly viscous medium.

The fluorescence lifetime and rotational correlation time of **71** were positively correlated with the viscosity.^{134,135} The viscosity in intracellular endocytic vesicles was determined to be 140 and 80 cP by fluorescence lifetime imaging (FLIM) and time-resolved fluorescence anisotropy measurements, respectively (Fig. 41). Kuimova and coworkers also reported the synthesis of **72** for mapping the viscosity in live-cell plasma membranes (Fig. 41).¹³⁶ Both membrane viscosity probes **71** and **72** have a long alkyl chain to be inserted into cell membranes. However, **71** could not avoid its internalization from the plasma membrane to intracellular vesicles via endocytosis. In contrast, **72** possesses a positive-charged tail that effectively prevents endocytic incorporation. As a result, the plasma membrane of the cells was exclusively stained with **72**, and its viscosity was determined to be 270 cP by FLIM imaging. Compared with endocytic vesicles, the plasma membrane possessed higher viscosity, which might reflect the lipid-rich environment in the plasma membrane.

To monitor the viscosity changes in lysosomes, molecular

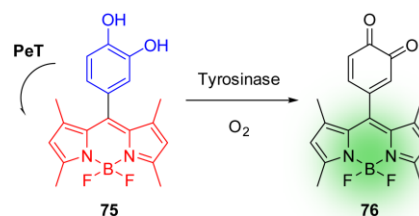


Fig. 42 BODIPY-based probe for visualization of tyrosinase activity.

rotor **73** was synthesized (Fig. 41).¹³⁷ A morpholine moiety was attached to BODIPY through a methylene linker for a lysosome-targeting group and a fluorescence turn-ON sensor based on a PeT mechanism. Lysosomal viscosity was measured as approximately 65 cP using FLIM, because the lifetime of **73** increased with increasing viscosity and was independent of pH. Moreover, **73** was applicable to real-time monitoring of lysosomal viscosity changes upon stimulation with dexamethasone, which causes membrane-stabilizing effects on lysosomes.¹³⁸

The viscosity in mitochondria was measured using coumarin-modified BODIPY **74**, which possesses a phosphonium moiety, as the mitochondria-targeting group, and the coumarinylphenyl group at the meso-position to form a molecular rotor structure (Fig. 41).¹³⁹ The fluorescence intensity of the BODIPY core at 516 nm was remarkably enhanced with increasing viscosity, whereas that of coumarin at 427 nm was almost independent of the viscosity. Therefore, the ratio of the two emission peaks was linearly correlated with the viscosity increase. These properties of **74** enabled it to perform ratiometric measurement of the mitochondrial viscosity of HeLa cells, which was calculated as 62.8 cP. Moreover, the treatment of ionophores, such as monensin and nystatin, raised the viscosity to 90.5 cP and 109 cP, respectively. This result indicates that the ionophores might induce structural changes or swelling of mitochondria,¹⁴⁰ leading to restriction of free rotation of the C-C bond at the meso-position.

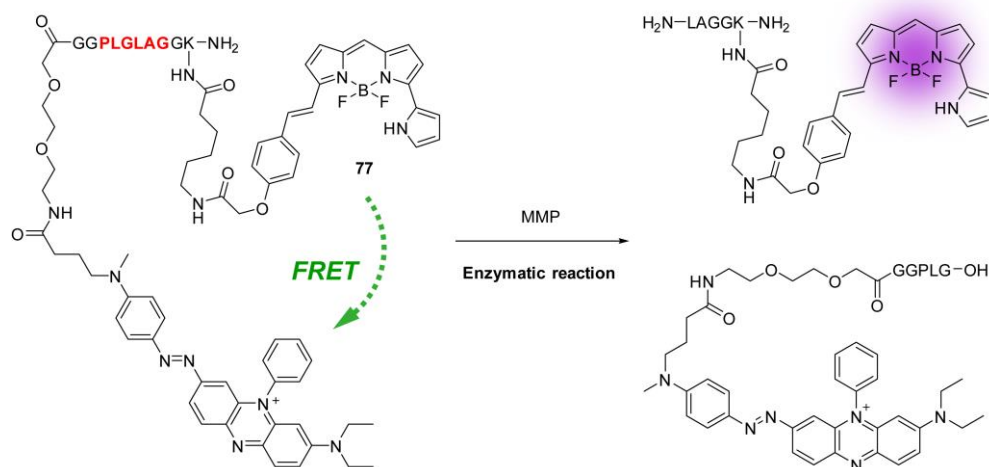


Fig. 43 FRET-based probe for MMP activity detection.

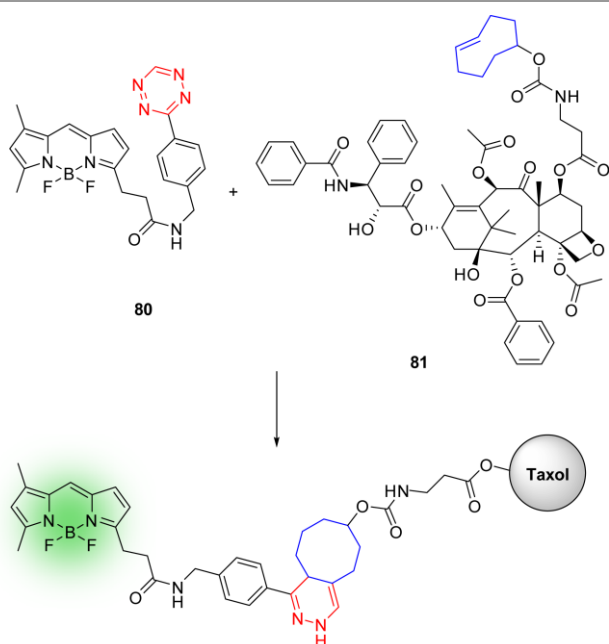


Fig. 46 BODIPY-labeled taxol via tetrazine-*trans*-cyclooctene ligation.

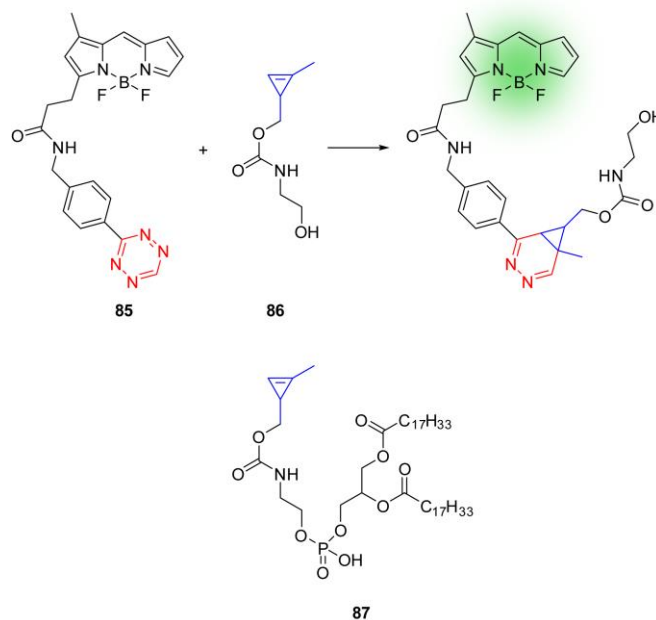


Fig. 48 Fluorogenic ligation of tetrazine-BODIPY **85** with cyclopropenes.

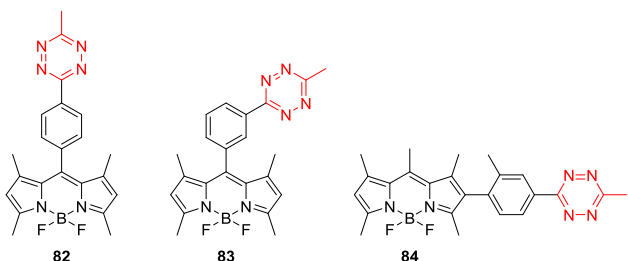


Fig. 47 BODIPY-tetrazine derivatives for investigation of quenching mechanisms.

fluorescence turn-ON ratio is dependent on the substitution position, and **83** produced the highest fold fluorescence increase (1600-fold). Changing the position of tetrazine from meta to para resulted in a lower turn-ON ratio (900-fold). In addition, the fluorescence intensity of **83** was independent of solvent polarity. From these results, it was suggested that FRET is not the sole reason for fluorescence quenching, and through-bond energy transfer appears to be associated to some extent, instead of PeT. However, the possibility of PeT involvement in this mechanism cannot be excluded, because PeT efficiency is strongly dependent on the interchromophore distance.¹⁵⁵ Therefore, further investigation into the quenching mechanism will be needed to fully understand these observations.

Bioorthogonal cycloaddition with tetrazine generally requires moderate-sized and highly-strained dienophiles, such as *trans*-cyclooctene, cyclooctyne, and norbornene.¹⁵⁶ To minimize the size of dienophile and improve its stability and reactivity, cyclopropene **86** was synthesized (Fig. 48).¹⁵⁷ In contrast to unsubstituted cyclopropene, which rapidly dimerizes at room temperature, cyclopropene **86** showed excellent stability in aqueous solution at 37 °C, as well as little reactivity with L-cysteine. The reaction of **86** with tetrazine-BODIPY **85** rapidly proceeded with a 22-fold fluorescence increase at 512

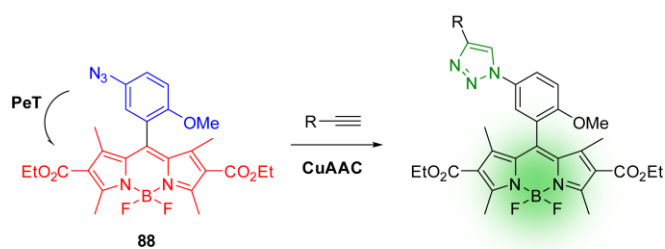


Fig. 49 Fluorogenic CuAAC reaction of azido-BODIPY.

nm. This fluorogenic cycloaddition was applied to live-cell imaging of cyclopropene phospholipid **87** bound on the membrane of SKBR3 human breast cancer cells (Fig. 48).

10-4. CuAAC

Wong and coworkers designed and synthesized azido-BODIPY **88** to obtain a fluorogenic probe for glycosylation (Fig. 49).¹⁵⁸ Although azido-BODIPY **88** showed almost no fluorescence, after transformation of the azide group to triazole by CuAAC reaction, termination of the fluorescence quenching occurred and produced a 52-fold fluorescence increase. The mechanism of fluorescence recovery can be explained by a-PeT, which was supported by density functional theory calculations. To incorporate an alkyne-tag into glycoproteins, CL1–5 lung cancer cells were treated with peracetylated alkynyl-*N*-acetylmannosamine (Ac₄ManNAI) or peracetylated alkynyl-*N*-acetylgalactosamine (Ac₄GalNAI). The fluorescence signals in Ac₄ManNAI-treated fixed cells were detected in the Golgi apparatus, whereas those in Ac₄GalNAI-treated fixed cells were mainly observed in the cytosol.

Conclusions & Perspectives

In this review, we summarized BODIPY-based fluorescent and fluorogenic probes that can be applied to cell and in vivo imaging. BODIPY fluorophores show remarkable optical properties, such as high fluorescence quantum yield, sharp emission, and high photostability. In addition, its fluorescence can be switched from OFF to ON in response to target molecules, analytes, and biological phenomena using FRET or PeT processes as quenching mechanisms. For that purpose, sophisticated probe design is required for specific visualization of target biomolecules. Such specific imaging will be achievable by considering the changes in molecular structure and frontier orbital energy level, which are induced by reaction with molecules of interest (e.g., as shown in **60**). Besides the simple turn-ON type detection, reversible fluorescence switching is desired for monitoring the dynamics of peptides, proteins, and cells. Fluorescent probes for cations, such as protons, calcium, and zinc, can reversibly detect their targets. Since reversible fluorescent probes can provide much more information about activity changes, interactions of biomolecules or cells, and concentration and localization of the target, their development will accelerate further understanding of biological systems.

Although the lipophilicity of BODIPY dyes may sometimes cause undesirable non-specific interactions with cellular components, their non-ionic property can promote further development of cell membrane-permeable probes to target intracellular biomolecules. Since membrane permeability depends on the entire structure of the probe, it can be hard to predict if negatively charged molecules are less or non-membrane-permeable (e.g., as shown in **15**). Thus, it can be efficient to consider the LogD value of probes.⁴⁰ Furthermore, as demonstrated for Fura-2-AM,¹⁵⁹ negatively charged probes with a carboxyl group can be loaded into cells by conversion to a membrane-permeable acetoxymethyl (AM) ester. The AM ester can be hydrolyzed by endogenous esterase to recover the initial carboxyl form,¹⁶⁰ leading to reduction of non-specific binding to intracellular biomolecules.

One possible application of BODIPY-based probes with relatively high intensity and photostability is for single-molecule and super-resolution microscopy,^{10,161,162} which are powerful techniques for visualizing and analyzing the localization and dynamics of individual proteins and biomolecules. So far, xanthene and cyanine dyes have been used for single-molecule imaging, and their photophysical properties and photochemical processes during light irradiation have been studied.^{163–166} On the other hand, there are few reports on single-molecule imaging in cells using BODIPY-based fluorescent probes.¹⁶⁷ Further studies on the photophysical and photochemical properties of BODIPY dye will provide useful information for developing fluorescent probes suitable for single-molecule imaging.

Additionally, further development of BODIPY-based probes for in vivo fluorescence imaging will be necessary. BODIPY dye could be a promising scaffold for in vivo

fluorescence imaging, because the emission wavelength of BODIPY dye can be tuned to the NIR region by chemical modification.^{26,168,169} Indeed, there is a gradually increasing number of reports on BODIPY-based probes applicable to in vivo studies and, in this review, we introduced several examples.^{73,79,84–86,88,115,144} Incorporation of cell- or tissue-specific targeting moieties to BODIPY-based NIR fluorescent probes will be required for further advances in the development of in vivo fluorescent probes.¹⁷⁰

Acknowledgements

This research was supported by the Ministry of Education, Culture, Sports, Science, and Technology, Japan (Grant Nos. 25620133, 25220207, and 26102529 to K.K., and 26•794 to H.M.), and by CREST from JST. The authors acknowledge the Asahi Glass Foundation and the Cosmetology Research Foundation.

References

1. C. J. Weijer, *Science*, 2003, **300**, 96.
2. B. N. G. Giepmans, S. R. Adams, M. H. Ellisman, R. Y. Tsien, *Science*, 2006, **312**, 217.
3. M. J. Pittet, R. Weissleder, *Cell*, 2011, **147**, 983.
4. R. N. Germain, E. A. Robey, M. D. Cahalan, *Science*, 2012, **336**, 1676.
5. J. Zhang, R. E. Campbell, A. Y. Ting, R. Y. Tsien, *Nat. Rev. Mol. Cell Biol.*, 2002, **3**, 906.
6. R. Y. Tsien, *Angew. Chem. Int. Ed.*, 2009, **48**, 5612.
7. R. H. Newman, M. D. Fosbrink, J. Zhang, *Chem. Rev.*, 2011, **111**, 3614.
8. J. Garcia-Bustos, J. Heitman, M. N. Hall, *Biochim. Biophys. Acta*, 1991, **1071**, 83.
9. B. Valeur, M. N. Berberan-Santos, *Molecular Fluorescence: Principles and Applications*, 2nd ed., Wiley-VCH, 2012.
10. M. Sauer, J. Hofkens, J. Enderlein, *Handbook of Fluorescence Spectroscopy and Imaging*, Wiley-VCH, 2011.
11. J. A. Prescher, C. R. Bertozzi, *Nat. Chem. Biol.*, 2005, **1**, 13.
12. R. K. V. Lim, Q. Lin, *Chem. Commun.*, 2006, **46**, 1589.
13. K. Lang, J. W. Chin, *ACS Chem. Biol.*, 2014, **9**, 16.
14. D. M. Patterson, L. A. Nazarova, J. A. Prescher, *ACS Chem. Biol.*, 2014, **9**, 592.
15. Y. Takaoka, A. Ojida, I. Hamachi, *Angew. Chem. Int. Ed.*, 2013, **52**, 4088.
16. T. Gronemeyer, G. Godin, K. Johnsson, *Curr. Opin. Chem. Biol.*, 2005, **16**, 453.
17. S. Mizukami, Y. Hori, K. Kikuchi, *Acc. Chem. Res.*, 2014, **47**, 247.
18. X. Li, X. Gao, W. Shi, H. Ma, *Chem. Rev.*, 2014, **114**, 590.
19. L. D. Lavis, R. T. Raines, *ACS Chem. Biol.*, 2008, **3**, 142.
20. L. M. Wsockia, L. D Lavis, *Curr. Opin. Chem. Biol.*, 2011, **15**, 752.
21. L. V. Johnson, M. L. Walsh, L. B. Chen, *Proc. Natl. Acad. Sci. USA*, 1980, **77**, 990.
22. J. O Escobedo, O. Rusin, S. Lim, R. M Strongin, *Curr. Opin. Chem. Biol.*, 2010, **14**, 64.
23. A. Loudet, K. Burgess, *Chem. Rev.*, 2007, **107**, 4891.

24. G. Ulrich, R. Ziessel, A. Harriman, *Angew. Chem. Int. Ed.*, 2008, **47**, 1184.
25. H. Lu, J. Mack, Y. Yanga, Z. Shen, *Chem. Soc. Rev.*, 2014, **43**, 4778.
26. Y. Ni, J. Wu, *Org. Biomol. Chem.*, 2014, **12**, 3774.
27. K. E. Sapsford, L. Berti, I. L. Medintz, *Angew. Chem. Int. Ed.*, 2006, **45**, 4562.
28. A. P. de Silva, H. Q. N. Gunaratne, T. Gunnlaugsson, A. J. M. Huxley, C. P. McCoy, J. T. Rademacher, T. E. Rice, *Chem. Rev.*, 1997, **97**, 1515.
29. H. Sunahara, Y. Urano, H. Kojima, T. Nagano, *J. Am. Chem. Soc.*, 2007, **129**, 5597.
30. H. Koutaka, J. Kosuge, N. Fukasaku, T. Hirano, K. Kikuchi, Y. Urano, H. Kojima, T. Nagano, *Chem. Pharm. Bull.*, 2004, **52**, 700.
31. Johnson, I., and M. T. Z. Spence., *The molecular probes handbook*, Life Technologies Corporation, 2010.
32. M. J. Culzoni, A. M. de la Peña, A. Machuca, H. C. Goicoechea, R. Babiano, *Anal. Methods.*, 2013, **5**, 30.
33. N. Boens, V. Leen, W. Dehaen, *Chem. Soc. Rev.*, 2012, **41**, 1130.
34. Q. Zheng, G. Xu, P. N. Prasad, *Chem. Eur. J.*, 2008, **14**, 5812.
35. L. Jiao, C. Yu, T. Uppal, M. Liu, Y. Li, Y. Zhou, E. Hao, X. Hu, M. G. H. Vicente, *Org. Biomol. Chem.*, 2010, **8**, 2517.
36. T. Uppal, X. Hu, F. R. Fronczek, S. Maschek, P. Bobadova-Parvanova, M. G. H. Vicente, *Chem. Eur. J.*, 2012, **18**, 3893.
37. X.-D. Jiang, R. Gao, Y. Yue, G.-T. Sun, W. Zhao, *Org. Biomol. Chem.*, 2012, **10**, 6861.
38. A. M. Courtis, S. A. Santos, Y. Guan, J. A. Hendricks, B. Ghosh, D. M. Szantai-Kis, S. A. Reis, J. V. Shah, R. Mazitschek, *Bioconjugate Chem.*, 2014, **25**, 1043.
39. J. A. Hendricks, E. J. Keliher, D. Wan, S. A. Hilderbrand, R. Weissleder, R. Mazitschek, *Angew. Chem. Int. Ed.*, 2012, **51**, 4603.
40. T. W. Johnson, K. R. Dress, M. Edwards, *Bioorg. Med. Chem. Lett.*, 2009, **19**, 5560.
41. Y. Ni, L. Zeng, N.-Y. Kang, K.-W. Huang, L. Wang, Z. Zeng, Y.-T. Chang, J. Wu, *Chem. Eur. J.*, 2014, **20**, 2301.
42. S. Zhang, T. Wu, J. Fan, Z. Li, N. Jiang, J. Wang, B. Dou, S. Sun, F. Song, X. Peng, *Org. Biomol. Chem.*, 2013, **11**, 555.
43. N. Jiang, J. Fan, T. Liu, J. Cao, B. Qiao, J. Wang, P. Gao, X. Peng, *Chem. Commun.*, 2013, **49**, 10620.
44. X. Zhang, Y. Xiao, J. Qi, J. Qu, B. Kim, X. Yue, K. D. Belfield, *J. Org. Chem.*, 2013, **78**, 9153.
45. B. C. Dickinson, D. Srikun, C. J. Chang, *Curr. Opin. Chem. Biol.*, 2010, **14**, 50.
46. M. J. Hinner, K. Johnsson, *Curr. Opin. Biotechnol.*, 2010, **21**, 766.
47. M. Vendrell, D. Zhai, J. C. Er, Y.-T. Chang, *Chem. Rev.*, 2012, **112**, 4391.
48. L.-G. Milroy, S. Rizzo, A. Calderon, B. Ellinger, S. Erdmann, J. Mondry, P. Verveer, P. Bastiaens, H. Waldmann, L. Dehmelt, H.-D. Arndt, *J. Am. Chem. Soc.*, 2012, **134**, 8480.
49. F. Gala, M. V. D'Auria, S. De Marino, V. Sepe, F. Zollo, C. D. Smith, S. N. Keller, A. Zampella, *Tetrahedron*, 2009, **65**, 51.
50. R. Tannert, L.-G. Milroy, B. Ellinger, T.-S. Hu, H.-D. Arndt, H. Waldmann, *J. Am. Chem. Soc.*, 2010, **132**, 3063.
51. P. A. Waghorn, M. W. Jones, A. McIntyre, A. Innocenti, D. Vullo, A. L. Harris, C. T. Supuran, J. R. Dilworth, *Eur. J. Inorg. Chem.*, 2012, 2898.
52. M. L. Vetter, Z. Zhang, S. Liu, J. Wang, H.Y. Cho, J. Zhang, W. Zhang, N. S. Gray, P. L. Yang, *ChemBioChem*, 2014, **15**, 1317.
53. S. K. V. Vernekar, H. Y. Hallaq, G. Clarkson, A. J. Thompson, L. Silvestri, S. C. R. Lummis, M. Lochner, *J. Med. Chem.*, 2010, **53**, 2324.
54. R. Weinstain, J. Kanter, B. Friedman, L. G. Ellies, M. E. Baker, R. Y. Tsien, *Bioconjugate Chem.*, 2013, **24**, 766.
55. N. G. Nørager, C. B. Jensen, M. Rathje, J. Andersen, K. L. Madsen, A. S. Kristensen, K. Strømgaard, *ACS Chem. Biol.*, 2013, **8**, 2033.
56. M. H. Poulsen, S. Lucas, T. B. Bach, A. F. Barlund, C. Wenzler, C. B. Jensen, A. S. Kristensen, K. Strømgaard, *J. Med. Chem.*, 2013, **56**, 1171.
57. J. Yang, H. Chen, I. R. Vlahov, J.-X. Cheng, P. S. Low, *Proc. Natl. Acad. Sci. USA*, 2006, **103**, 13872.
58. F. Kotzyba-Hibert, I. Kapfer, M. Goeldner, *Angew. Chem. Int. Ed.*, 1995, **34**, 1296.
59. L. Dubinsky, B. P. Krom, M. M. Meijler, *Bioorg. Med. Chem.*, 2012, **20**, 554.
60. X. Li, J.-H. Cao, Y. Li, P. Rondard, Y. Zhang, P. Yi, J.-F. Liu, F.-J. Nan, *J. Med. Chem.*, 2008, **51**, 3057.
61. K. Kaupmann, K. Huggel, J. Heid, P. J. Flor, S. Bischoff, S. J. Mickel, G. McMaster, C. Angst, H. Bittiger, W. Froestl, B. Bettler, *Nature*, 1997, **386**, 239.
62. D. A. Bachovchin, B. F. Cravatt, *Nat. Rev. Drug Discov.*, 2012, **11**, 52.
63. M. J. Evans, B. F. Cravatt, *Chem. Rev.*, 2006, **106**, 3279.
64. J. Z. Long, W. Li, L. Booker, J. J. Burston, S. G. Kinsey, J. E. Schlosburg, F. J. Pavón, A. M. Serrano, D. E. Selley, L. H. Parsons, A. H. Lichtman, B. F. Cravatt, *Nat. Chem. Biol.*, 2009, **5**, 37.
65. J. W. Chang, A. B. Cognetta, III, M. J. Niphakis, B. F. Cravatt, *ACS Chem. Biol.*, 2013, **8**, 1590.
66. K.-L. Hsu, K. Tsuboi, A. Adibekian, H. Pugh, K. Masuda, B. F. Cravatt, *Nat. Chem. Biol.*, 2012, **8**, 999.
67. L. W. Miller, Y. Cai, M. P. Sheetz, V. W. Cornish, *Nat. Methods*, 2005, **2**, 255.
68. W. Liu, F. Li, X. Chen, J. Hou, L. Yi, Y.-W. Wu, *J. Am. Chem. Soc.*, 2014, **136**, 4468.
69. J.-J. Lee, S.-C. Lee, D. Zhai, Y.-H. Ahn, H. Y. Yeo, Y. L. Tana, Y.-T. Chang, *Chem. Commun.*, 2011, **47**, 4508.
70. C. Brieke, F. Rohrbach, A. Gottschalk, G. Mayer, A. Heckel, *Angew. Chem. Int. Ed.*, 2012, **51**, 8446.
71. G. Bort, T. Gallavardin, D. Ogden, P. I. Dalko, *Angew. Chem. Int. Ed.*, 2013, **52**, 4526.
72. A. Keppler, S. Gendreizig, T. Gronemeyer, H. Pick, H. Vogel, K. Johnsson, *Nat. Biotechnol.*, 2003, **21**, 86.
73. T. Kobayashi, T. Komatsu, M. Kamiya, C. Campos, M. González-Gaitán, T. Terai, K. Hanaoka, T. Nagano, Y. Urano, *J. Am. Chem. Soc.*, 2012, **134**, 11153.
74. G. R. Rosania, J. W. Lee, L. Ding, H.-S. Yoon, Y.-T. Chang, *J. Am. Chem. Soc.*, 2003, **125**, 1130.
75. J.-S. Lee, M. Vendrell, Y.-T. Chang, *Curr. Opin. Chem. Biol.*, 2011, **15**, 760.
76. J.-S. Lee, N.-y. Kang, Y. K. Kim, A. Samanta, S. Feng, H. K. Kim, M. Vendrell, J. H. Park, Y.-T. Chang, *J. Am. Chem. Soc.*, 2009, **131**, 10077.

77. Y. M. Cho, Y. Fujita, T. J. Kieffer, *Annu. Rev. Physiol.*, 2014, **76**, 535.
78. S.-W. Yuna, C. Leong, D. Zhai, Y. L. Tan, L. Lim, X. Bi, J.-J. Lee, H. J. Kim, N.-Y. Kang, S. H. Ng, L. W. Stanton, Y.-T. Chang, *Proc. Natl. Acad. Sci. USA*, 2012, **109**, 10214.
79. N.-Y. Kang, S.-C. Lee, S.-J. Park, H.-H. Ha, S.-W. Yun, E. Kostromina, N. Gustavsson, Y. Ali, Y. Chandran, H.-S. Chun, M. A. Bae, J. H. Ahn, W. Han, G. K. Radda, Y.-T. Chang, *Angew. Chem. Int. Ed.*, 2013, **52**, 8557.
80. J. R. Casey, S. Grinstein, J. Orłowski, *Nat. Rev. Mol. Cell Biol.*, 2010, **11**, 50.
81. T. Gareis, C. Huber, O. S. Wolfbeis, J. Daub, *Chem. Commun.*, 1997, 1717.
82. M. Kollmannsberger, T. Gareis, S. Heintl, J. Breu, J. Daub, *Angew. Chem. Int. Ed.*, 1997, **36**, 1333.
83. T. Werner, C. Huber, S. Heintl, M. Kollmannsberger, J. Daub, O. S. Wolfbeis, *Fresenius J. Anal. Chem.*, 1997, **359**, 150.
84. Y. Urano, D. Asanuma, Y. Hama, Y. Koyama, T. Barrett, M. Kamiya, T. Nagano, T. Watanabe, A. Hasegawa, P. L. Choyke, H. Kobayashi, *Nat. Med.*, 2009, **15**, 104.
85. T. Kowada, J. Kikuta, A. Kubo, M. Ishii, H. Maeda, S. Mizukami, K. Kikuchi, *J. Am. Chem. Soc.*, 2011, **133**, 17772.
86. J. Kikuta, Y. Wada, T. Kowada, Z. Wang, G.-H. Sun-Wada, I. Nishiyama, S. Mizukami, N. Maiya, H. Yasuda, A. Kumanogoh, K. Kikuchi, R. N. Germain, M. Ishii, *J. Clin. Invest.*, 2013, **123**, 866.
87. S. Hoogendoorn, K. L. Habets, S. Passemard, J. Kuiper, G. A. van der Marel, B. I. Florea, H. S. Overkleeft, *Chem. Commun.*, 2011, **47**, 9363.
88. A. Vázquez-Romero, N. Kielland, M. J. Arévalo, S. Preciado, R. J. Mellanby, Y. Feng, R. Lavilla, M. Vendrell, *J. Am. Chem. Soc.*, 2013, **135**, 16018.
89. C. C. Winterbourn, M. B. Hampton, *Free Radic. Biol. Med.*, 2008, **45**, 549.
90. S. C. Lu, *Mol. Asp. Med.*, 2009, **30**, 42.
91. H. S. Jung, X. Chen, J. S. Kim, J. Yoon, *Chem. Soc. Rev.*, 2013, **42**, 6019.
92. X. Li, S. Qian, Q. He, B. Yang, J. Li, Y. Hu, *Org. Biomol. Chem.*, 2010, **8**, 3627.
93. H. Guo, Y. Jing, X. Yuan, S. Ji, J. Zhao, X. Li, Y. Kan, *Org. Biomol. Chem.*, 2011, **9**, 3844.
94. J. Shao, H. Guo, S. Ji, J. Zhao, *Biosens. Bioelectron.*, 2011, **26**, 3012.
95. J. Shao, H. Sun, H. Guo, S. Ji, J. Zhao, W. Wu, X. Yuan, C. Zhang, T. D. James, *Chem. Sci.*, 2012, **3**, 1049.
96. L.-Y. Niu, Y.-S. Guan, Y.-Z. Chen, L.-Z. Wu, C.-H. Tung, Q.-Z. Yang, *J. Am. Chem. Soc.*, 2012, **134**, 18928.
97. H. P. Burchfield, *Nature*, 1958, **181**, 49.
98. H. Kondo, F. Moriuchi, J. Sunamoto, *J. Org. Chem.*, 1981, **46**, 1333.
99. L.-Y. Niu, Y.-S. Guan, Y.-Z. Chen, L.-Z. Wu, C.-H. Tung, Q.-Z. Yang, *Chem. Commun.*, 2013, **49**, 1294.
100. S. Madhu, R. Gonnade, M. Ravikanth, *J. Org. Chem.*, 2013, **78**, 5056.
101. M. Işık, R. Guliyev, S. Kolemen, Y. Altay, B. Senturk, T. Tekinay, E. U. Akkaya, *Org. Lett.*, 2014, **16**, 3260.
102. M. Zhang, Y. Wu, S. Zhang, H. Zhu, Q. Wu, L. Jiao, E. Hao, *Chem. Commun.*, 2012, **48**, 8925.
103. L. Long, W. Lin, B. Chen, W. Gao, L. Yuan, *Chem. Commun.*, 2011, **47**, 893.
104. P. E. Dawson, T. W. Muir, I. Clark-Lewis, S. B. H. Kent, *Science*, 1994, **266**, 776.
105. J. S. Stamler, *Cell*, 1994, **78**, 931.
106. C. Szabó, *Nat. Rev. Drug Discov.*, 2007, **6**, 917.
107. A. K. Mustafa, M. M. Gadalla, S. H. Snyder, *Sci. Signal.*, 2009, **2**, re2.
108. Y. Qian, J. Karpus, O. Kabil, S.-Y. Zhang, H.-L. Zhu, R. Banerjee, J. Zhao, C. He, *Nat. Commun.*, 2011, **2**, 495.
109. S. Singh, D. Padovani, R. A. Leslie, T. Chiku, R. Banerjee, *J. Biol. Chem.*, 2009, **284**, 22457.
110. X. Cao, W. Lin, K. Zheng, L. He, *Chem. Commun.*, 2012, **48**, 10529.
111. A. R. Lippert, E. J. New, C. J. Chang, *J. Am. Chem. Soc.*, 2011, **133**, 10078.
112. H. Peng, Y. Cheng, C. Dai, A. L. King, B. L. Predmore, D. J. Lefler, B. Wang, *Angew. Chem. Int. Ed.*, 2011, **50**, 9672.
113. T. Saha, D. Kand, P. Talukdar, *Org. Biomol. Chem.*, 2013, **11**, 8166.
114. Y. Gabe, Y. Urano, K. Kikuchi, H. Kojima, T. Nagano, *J. Am. Chem. Soc.*, 2004, **126**, 3357.
115. H.-X. Zhang, J.-B. Chen, X.-F. Guo, H. Wang, H.-S. Zhang, *Anal. Chem.*, 2014, **86**, 3115.
116. T. Wang, E. F. Douglass, Jr., K. J. Fitzgerald, D. A. Spiegel, *J. Am. Chem. Soc.*, 2013, **135**, 12429.
117. B. W. Michel, A. R. Lippert, C. J. Chang, *J. Am. Chem. Soc.*, 2012, **134**, 15668.
118. J. Nordberg, E. S. J. Arnér, *Free Radic. Biol. Med.*, 2001, **31**, 1287.
119. F. C. Fang, *Nat. Rev. Microbiol.*, 2004, **2**, 820.
120. Z.-N. Sun, F.-Q. Liu, Y. Chen, P. K. H. Tam, D. Yang, *Org. Lett.*, 2008, **10**, 2171.
121. J. J. Hu, N.-K. Wong, Q. Gu, X. Bai, S. Ye, D. Yang, *Org. Lett.*, 2014, **16**, 3544.
122. S.-R. Liu, S.-P. Wu, *Org. Lett.*, 2013, **15**, 878.
123. B. Wang, P. Li, F. Yu, P. Song, X. Sun, S. Yang, Z. Lou, K. Han, *Chem. Commun.*, 2013, **49**, 1014.
124. B. Wang, P. Li, F. Yu, J. Chen, Z. Qu, K. Han, *Chem. Commun.*, 2013, **49**, 5790.
125. M. Emrullahoğlu, M. Üçüncü, E. Karakuş, *Chem. Commun.*, 2013, **49**, 7836.
126. S. T. Manjare, S. Kim, W. D. Heo, D. G. Churchill, *Org. Lett.*, 2014, **16**, 410.
127. A. Khatchadourian, K. Krumova, S. Boridy, A. T. Ngo, D. Maysinger, G. Cosa, *Biochemistry*, 2009, **48**, 5658.
128. K. Krumova, L. E. Greene, G. Cosa, *J. Am. Chem. Soc.*, 2013, **135**, 17135.
129. K. Krumova, P. Oleynik, P. Karam, G. Cosa, *J. Org. Chem.*, 2009, **74**, 3641.
130. D. Yang, M.-K. Wong, Z. Yan, *J. Org. Chem.*, 2000, **65**, 4179.
131. D. Yang, H.-L. Wang, Z.-N. Sun, N.-W. Chung, J.-G. Shen, *J. Am. Chem. Soc.*, 2006, **128**, 6004.
132. Z.-N. Sun, H.-L. Wang, F.-Q. Liu, Y. Chen, P. Kwong, H. Tam, D. Yang, *Org. Lett.*, 2009, **11**, 1887.

133. E. O. Puchkov, *Biochem. (Mosc.) Suppl. Ser. A Membr. Cell Biol.*, 2013, **7**, 270.
134. M. K. Kuimova, G. Yahiolglu, J. A. Levitt, K. Suhling, *J. Am. Chem. Soc.*, 2008, **130**, 6672.
135. J. A. Levitt, M. K. Kuimova, G. Yahiolglu, P.-H. Chung, K. Suhling, D. Phillips, *J. Phys. Chem. C*, 2009, **113**, 11634.
136. I. López-Duarte, T. T. Vu, M. A. Izquierdo, J. A. Bull, M. K. Kuimova, *Chem. Commun.*, 2014, **50**, 5282.
137. L. Wang, Y. Xiao, W. Tian, L. Deng, *J. Am. Chem. Soc.*, 2013, **135**, 2903.
138. B. Hinz, R. Hirschelmann, *Pharm. Res.*, 2000, **17**, 1489.
139. Z. Yang, Y. He, J.-H. Lee, N. Park, M. Suh, W.-S. Chae, J. Cao, X. Peng, H. Jung, C. Kang, J. S. Kim, *J. Am. Chem. Soc.*, 2013, **135**, 9181.
140. S. P. Soltoff, L. J. Mandel, *J. Membrane Biol.*, 1986, **94**, 153.
141. T.-I. Kim, J. Park, S. Park, Y. Choi, Y. Kim, *Chem. Commun.*, 2011, **47**, 12640.
142. C. A. Ramsden, P. A. Riley, *Bioorg. Med. Chem.*, 2014, **22**, 2388.
143. T. Myochin, K. Hanaoka, T. Komatsu, T. Terai, T. Nagano, *J. Am. Chem. Soc.*, 2012, **134**, 13730.
144. K. E. Linder, E. Metcalfe, P. Nanjappan, T. Arunachalam, K. Ramos, T. M. Skedzielewski, E. R. Marinelli, M. F. Tweedle, A. D. Nunn, R. E. Swenson, *Bioconjugate Chem.*, 2011, **22**, 1287.
145. S. S. van Berkel, M. B. van Eldijk, J. C. M. van Hest, *Angew. Chem. Int. Ed.*, 2011, **50**, 8806.
146. E. Lallana, R. Riguera, E. Fernandez-Megia, *Angew. Chem. Int. Ed.*, 2011, **50**, 8794.
147. J. C. Jewett, C. R. Bertozzi, *Chem. Soc. Rev.*, 2010, **39**, 1272.
148. J. Rayo, N. Amara, P. Krief, M. M. Meijler, *J. Am. Chem. Soc.*, 2011, **133**, 7469.
149. Y. Zeng, T. N. C. Ramya, A. Dirksen, P. E. Dawson, J. C. Paulson, *Nat. Methods*, 2009, **6**, 207.
150. K. E. Beatty, J. Szychowski, J. D. Fisk, D. A. Tirrell, *ChemBioChem*, 2011, **12**, 2137.
151. K. L. Kiick, E. Saxon, D. A. Tirrell, C. R. Bertozzi, *Proc. Natl. Acad. Sci. USA*, 2002, **99**, 19.
152. N. K. Devaraj, S. Hilderbrand, R. Upadhyay, R. Mazitschek, R. Weissleder, *Angew. Chem. Int. Ed.*, 2010, **49**, 2869.
153. C. Dumas-Verdes, F. Miomandre, E. Lépicier, O. Galangau, T. T. Vu, G. Clavier, R. Méallet-Renault, Pierre Audebert, *Eur. J. Org. Chem.*, 2010, 2525.
154. J. C. T. Carlson, L. G. Meimetis, S. A. Hilderbrand, R. Weissleder, *Angew. Chem. Int. Ed.*, 2013, **52**, 6917.
155. T. Matsumoto, Y. Urano, T. Shoda, H. Kojima, T. Nagano, *Org. Lett.*, 2007, **9**, 3375.
156. W. Chen, D. Wang, C. Dai, D. Hamelberg, B. Wang, *Chem. Commun.*, 2012, **48**, 1736.
157. J. Yang, J. Šečutè, C. M. Cole, N. K. Devaraj, *Angew. Chem. Int. Ed.*, 2012, **51**, 7476.
158. J.-J. Shie, Y.-C. Liu, Y.-M. Lee, C. Lim, J.-M. Fang, C.-H. Wong, *J. Am. Chem. Soc.*, 2014, **136**, 9953.
159. R. Y. Tsien, T. J. Rink, M. Poenie, *Cell Calcium*, 1985, **6**, 145.
160. R. Y. Tsien, *Nature*, 1981, **290**, 527.
161. W. E. Moerner, T. Basché, *Angew. Chem. Int. Ed.*, 1993, **32**, 457.
162. S. W. Hell, *Science*, 2007, **316**, 1153.
163. M. Fernández-Suárez, A. Y. Ting, *Nat. Rev. Mol. Cell Biol.*, 2008, **9**, 929.
164. S. J. Lord, H.-I. D. Lee, W. E. Moerner, *Anal. Chem.*, 2010, **82**, 2192.
165. S. van de Linde, A. Löschberger, T. Klein, M. Heidbreder, S. Wolter, M. Heilemann, M. Sauer, *Nat. Protoc.*, 2011, **6**, 991.
166. E. M. S. Stennett, M. A. Ciuba, M. Levitus, *Chem. Soc. Rev.*, 2014, **43**, 1057.
167. S.-H. Shima, C. Xia, G. Zhong, H. P. Babcock, J. C. Vaughan, B. Huang, X. Wang, C. Xu, G.-Q. Bi, X. Zhuang, *Proc. Natl. Acad. Sci. USA*, 2012, **109**, 13978.
168. K. Umezawa, D. Citterio, K. Suzuki, *Anal. Sci.*, 2014, **30**, 327.
169. L. Yuan, W. Lin, K. Zheng, L. He, W. Huang, *Chem. Soc. Rev.*, 2013, **42**, 622.
170. S. A. Hilderbrand, R. Weissleder, *Curr Opin. Chem. Biol.*, 2010, **14**, 71.